JCI The Journal of Clinical Investigation

Graft IL-33 regulates infiltrating macrophages to protect against chronic rejection

Tengfang Li, … , Stephen F. Badylak, Heth R. Turnquist

J Clin Invest. 2020. https://doi.org/10.1172/JCI133008.

Research In-Press Preview Immunology Transplantation

Graphical abstract

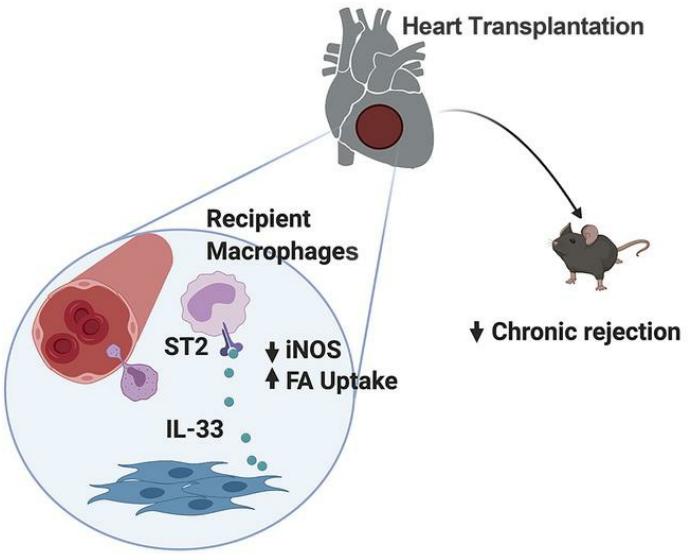

Graft IL-33 regulates infiltrating macrophages to protect against chronic rejection

Tengfang Li[1,2,3,*], Zhongqiang Zhang[1,2,4,*], Joe G. Bartolacci[1,5], Gaelen K. Dwyer[1,2,6], Quan Liu[1,2,7], Lisa R. Mathews[1,2], Murugesan Velayutham[1,2,8,9], Anna S. Roessing[1,2,6], Yoojin C. Lee[5,10], Helong Dai[1,2,3], Sruti Shiva[8,9], Martin H. Oberbarnscheidt[1,2,6], Jenna L. Dziki[1,5], Steven J. Mullet[10,11,12], Stacy G. Wendell[9,10,11,12], James D. Wilkinson[13], Steven A. Webber[13], Michelle Wood-Trageser[2,14], Simon C. Watkins[15], Anthony J. Demetris[2,5,14], George S. Hussey[1,5], Stephen F. Badylak[1,5,10], and Hēth R. Turnquist[1,2,5,6]

[1]Department of Surgery, University of Pittsburgh School of Medicine, Pittsburgh, PA, USA. [2]Thomas E. Starzl Transplantation Institute, University of Pittsburgh School of Medicine, Pittsburgh, PA, USA. [3]Department of Kidney Transplantation, The Second Xiangya Hospital of Central South University, Changsha, China. [4]Department of Organ Transplantation and General Surgery, The Second Xiangya Hospital of Central South University, Changsha, China. [5]McGowan Institute for Regenerative Medicine, University of Pittsburgh, Pittsburgh, PA, USA. [6]Department of Immunology, University of Pittsburgh, Pittsburgh, PA, USA. [7]Southern University of Science and Technology, Shenzhen, China. [8]Pittsburgh Heart, Lung, and Blood, Vascular Medicine Institute and [9]Department of Pharmacology and Chemical Biology, University of Pittsburgh School of Medicine, Pittsburgh, PA, USA. [10]Department of Bioengineering, University of Pittsburgh, Pittsburgh, PA, USA. [11]Health Sciences Metabolomics and Lipidomics Core, Pittsburgh, PA, USA. [12]Clinical Translational Science Institute, University of Pittsburgh, Pittsburgh, PA, USA. [13]Department of Pediatrics, Vanderbilt School of Medicine, Nashville, TN, USA. [14]Department of Pathology, University of Pittsburgh School of Medicine, Pittsburgh, PA, USA. [15]Department of Cell Biology, University of Pittsburgh, Pittsburgh, PA, USA.

[*]These authors share the first-author position as each contributed key data to the manuscript. The final order was determined based on the work contributed in the laboratory and in manuscript preparation with T. Li contributing the most followed by Z. Zhang.

Corresponding author: Heth R. Turnquist (het5@pitt.edu), E1554 Biomedical Science Tower, 200 Lothrop Street, Pittsburgh, PA 15261, USA. Phone: 412-624-6695.

Competing Interests statement: SFB, JLD, and GSH are shareholders in ECM-Therapeutics, Inc. JLD, ZZ, GSH, SFB, HRT, QL are listed inventors on patent application PCT/US2019/030547 ("MATRIX BOUND VESICLES (MBVS) CONTAINING IL-33 AND THEIR USE").

ABSTRACT

Alarmins, sequestered self-molecules containing damage-associated molecular patterns, are released during tissue injury to drive innate immune cell pro-inflammatory responses. Whether endogenous negative regulators controlling early immune responses are also released at the site of injury is poorly understood. Herein, we establish that the stromal cell-derived alarmin interleukin-33 (IL-33) is a local factor that directly restricts the pro-inflammatory capacity of graft infiltrating macrophages early after transplantation. By assessing heart transplant recipient samples and using a mouse heart transplant model, we establish that IL-33 is upregulated in allografts to limit chronic rejection. Mouse cardiac transplants lacking IL-33 displayed dramatically accelerated vascular occlusion and subsequent fibrosis, which was not due to altered systemic immune responses. Instead, a lack of graft IL-33 caused local augmentation of pro-inflammatory $iNOS^+$ macrophages that accelerated graft loss. IL-33 facilitated a metabolic program in macrophages associated with reparative and regulatory functions, and local delivery of IL-33 prevented the chronic rejection of IL-33-deficient cardiac transplants. Therefore, IL-33 represents a novel regulatory alarmin in transplantation that limits chronic rejection by restraining the local activation of pro-inflammatory macrophages. The local delivery of IL-33 in extracellular matrix based-based materials may be a promising biologic for chronic rejection prophylaxis.

INTRODUCTION

Acute heart transplant rejection can typically be averted by immunosuppressant therapy, which controls recipient $CD4^+$ and $CD8^+$ T cell responses to polymorphic amino acids in donor MHC molecules or donor-derived peptides presented in recipient MHC (1, 2). However, immunosuppressants are ineffective against development of chronic heart transplant rejection, a progressive vascular and fibrotic remodeling that leads to progressive myocardial dysfunction and loss of the majority of grafts within approximately 11 years post-transplant (3-5). While the immunopathology of chronic rejection is not fully understood, experimental studies have clearly established that chronic rejection of heart transplants, manifesting as vessel occlusion and myocardial fibrosis, is an immunologically-driven process that does not occur in the absence of adaptive immune cells, particularly T cells (6). Clinical studies have indicated the importance of alloimmune response to Human Leukocyte Antigen (HLA), as patients transplanted with cardiac grafts with HLA mismatching are reported to have higher incidence of chronic allograft vasculopathy (CAV), with HLA-DR mismatching being the most important HLA subtype (7, 8). The number of acute rejection episodes and total rejection score are positively related to development of CAV in both human and animal models (9, 10). Anti-HLA and anti-endothelial antibodies are also implicated in development of CAV (11, 12).

While chronic rejection is T and B cell-mediated, innate immune cells, including natural killer (NK) cells, inflammatory macrophages, monocytes, and monocyte-derived dendritic cells (monoDC), initiate and sustain the adaptive responses leading to chronic rejection. Chronic heart rejection does not occur in $RAG^{-/-}$ mice lacking T and B cells, yet NK cells predisposed allografts to adoptively-transferred, T cell-mediated chronic rejection (13). Likewise, kidney and heart allografts are rapidly infiltrated with recipient monocytes that differentiate into inflammatory macrophages and monoDC, which act as a critical local stimuli to alloreactive T cells (14). Early macrophage depletion (15) and targeting macrophage mTOR signaling (16, 17) suppresses cardiac allograft vasculopathy in mice. Given that T cell centric immunosuppressants fail to

prevent chronic rejection, the development of new therapeutics able to limit the early response of innate immune cells after transplant surgery may be an effective tool to improve long-term outcomes after HTx which have not changed significantly in the last 20 years (5).

It is well appreciated in transplantation that ischemia–reperfusion injury (IRI) arising after abrupt disruption and re-establishment of the blood supply to the solid organ results in myeloid cell infiltration, differentiation, and pro-inflammatory activation in the graft (18). Like IRI, surgical procedures, recipient conditioning, or alloimmune responses also cause tissue damage or non-apoptotic cell death that releases sequestered self-derived molecules, or "alarmins", to alert the immune system (18). There have been numerous pro-inflammatory alarmins identified, such as ATP, mitochondrial contents, and DNA. However, the best characterized alarmin is high-mobility group box 1 (HMGB1) (18). HMGB1 stimulates myeloid cells through TLR4 and RAGE to promote the expression of co-stimulatory molecules and pro-inflammatory cytokines. These mechanisms have been shown to support acute and chronic rejection in experimental models (16, 18-20) and implicated clinically in acute liver graft rejection (21) and chronic heart transplant rejection (22). HMGB1 is upregulated by IRI in cadaveric kidney transplants, but absent in living donor grafts and recipients having a TLR4 mutation decreasing the affinity for HMGB1 have higher rates of immediate graft function (23). This finding is also consistent with the observation that despite HLA mismatch, recipients of live, unrelated donor kidneys have significantly better long-term outcomes relative to those receiving HLA-matched cadaveric kidney grafts subjected to longer periods of ischemia (24). Recently it was shown that HMGB1 upregulated in mouse cardiac tissue following IRI, induces a metabolic profile and epigenetic modification in myeloid cells that supports pro-inflammatory cytokine secretion (16). Inhibition of HMGB1-augmented glycolysis using mTOR inhibition directed to myeloid cells using nanovesicles prolonged allograft survival (16). Thus, ischemic injury releasing pro-inflammatory alarmins sets the stage for long term outcomes through actions on myeloid cells.

However, there is limited evidence that not all alarmins are pro-inflammatory and some may actually have beneficial functions after transplantation by stimulating tissue repair or supporting immune regulation (25). IL-33 is an IL-1 family member and alarmin that is typically sequestered in the nucleus (26) or extracellular-matrix (ECM) of stromal cells (27). When released after tissue damage, IL-33 signals to immune cells via the IL-33 receptor IL-1R-like-1(IL1RL1), more commonly referred to as Stimulation-2 (ST2) (26). Our work, and that of others, has shown that administration of recombinant (r)IL-33 post-heart transplantation prolongs allograft survival across MHC barriers in rodent heart transplant models (28, 29). In further studies, we established that a dominant mechanism of action supporting the therapeutic benefit of rIL-33 was immune regulation through systemic expansion of $ST2^+$ Treg (29, 30). IL-33 expressed by fibro/adipogenic progenitors in the skeletal muscle has also been shown to regulate skeletal muscle Treg homeostasis and support muscle regeneration (31). Related studies have suggested a direct, cardiac protective role for rIL-33 against hypertrophy resulting from cardiac overload (32) and fibrosis after myocardial infarction (33). However, delivery of rIL-33 also aggravates autoimmune eosinophilic pericarditis during coxsackievirus B3 infection (34), suggesting that IL-33 can contribute to cardiac inflammation. IL-33 expression has been reported in cardiac fibroblasts (32) and the vasculature (35), yet how the expression of this alarmin is modulated in cardiac allografts or impacts outcomes was unknown.

Using IL-33 deficient heart grafts in a mouse chronic rejection model we have established that IL-33 stands out among identified alarmins and limits differentiation of pro-inflammatory macrophages to prevent chronic rejection. Specifically, transplants lacking IL-33 displayed dramatically accelerated chronic rejection-associated vasculopathy and subsequent fibrosis orchestrated by graft infiltrating recipient pro-inflammatory macrophages. IL-33-expressing heart grafts in recipients with ST2-deficient macrophages also displayed increased graft infiltration by pro-inflammatory macrophages and accelerated graft loss. Mechanistic studies demonstrated that IL-33 promoted a reparative macrophage phenotype through a metabolic reprograming

involving augmented oxidative phosphorylation (OXHPOS) and fatty acid (FA) uptake. We also revealed that IL-33 prevents pro-inflammatory stimuli-induced disruption of the tricarboxylic acid (TCA) cycle that shifts macrophage metabolism to anaerobic glycolysis and generates pro-inflammatory metabolites (36, 37). Restoration of IL-33 to IL-33-deficient heart transplants using vesicles in extracellular matrix (ECM)-derived hydrogel immediately after transplantation profoundly reduced the frequency of pro-inflammatory myeloid cells in the graft and prevented graft loss to chronic rejection. Thus, the local delivery of IL-33 in ECM-based materials after transplantation may be a practical and promising biologic for chronic rejection prophylaxis.

RESULTS

IL-33 is augmented in the allograft and circulation during heart transplant rejection.

To define how endogenous IL-33 shapes cardiac transplantation outcomes, we crossed C57BL/6 (B6) IL-33 knockout mice (38) onto the B6 H2-Ab1^{Bm12} (Bm12) background. Bm12 mice are a 'variant' strain of B6 mice in which a spontaneous mutation in third hypervariable region of the beta 1 domain results in alteration of 3 amino acids to generate a distinct I-A molecule, I-A^{bm12} (39). When transplanted into B6 mice, this MHCII molecule is recognized by alloreactive immune cells, particularly CD4$^+$ T cells. These responses do not typically result in early acute rejection of Bm12 allografts, but instead result in chronic rejection-associated fibrosis and vasculopathy in contracting grafts at late time points (>30-100 days post-transplant) (40, 41). In using this model, we were able to assess the impact of IL-33 upon the alloimmune responses shaping chronic rejection in the absence of immunosuppression.

When *il33*$^{-/-}$ Bm12 and *il33*$^{+/+}$ Bm12 hearts were transplanted into *il33*$^{+/+}$ B6 recipients and assessed using quantitative Immunofluorescence (IF) on post-operative day (POD)3 and 94, we found a rapid increase in IL-33$^+$ cells that was sustained above baseline levels throughout the life of the transplant (**Figure 1A-B** and **Supplemental Data Figure 1**). Consistent with other reports (31, 42), graft IL-33$^+$ cells were predominantly CD45$^-$ Vimentin$^+$ stromal cells. Interestingly, while *il33*$^{-/-}$ Bm12 IL-33 KO grafts lack IL-33$^+$ cells at POD3, there was a small fraction of CD45$^-$ IL-33$^+$ cells at late timepoints. These data suggest that recipient-derived cells, most likely fibrocytes (43, 44), can also contribute IL-33 to the transplant microenvironment. While IL-33$^+$ leukocytes have been described (26), there was a lack of evidence for significant CD45$^+$ IL-33$^+$ leukocytes in the transplanted grafts (**Figure 1A**).

We next assessed if a similar modulation of IL-33 was observed clinically by quantitating the level of IL-33 expressed in endomyocardial biopsies (EMB) and circulating in the serum of pediatric heart transplant recipients. Comparing the expression of IL-33 in EMB in the first year after transplant at times of pathologist-diagnosed acute cellular rejection (ACR; ISHLT grade $\geq$2R)

or antibody mediated rejection (AMR ≥2) episodes to those that were deemed rejection-free revealed that periods of diagnosed clinical rejection were associated with increased IL-33^{+} cells in the graft (**Figure 1C-D**). Thus, these data paralleled the above findings in our rodent heart transplant model. IL-33 levels were also compared between EMB from recipients suffering severe or mild chronic rejection-associated coronary artery vasculopathy (CAV) at least 300 days post-transplant. These limited data suggested that those with more severe CAV had decreased levels of IL-33 (**Figure 1C-D**). Assessment of recipient serum revealed that there was a large increase in circulating IL-33 in recipients suffering a diagnosed early rejection event compared to recipients deemed rejection-free during a similar time period, which were similar to normal levels (**Figure 1E**). Later timepoints also showed a return to normal IL-33 levels, including serum from recipients with severe CAV (**Figure 1E**). In total, these data showed that endogenous IL-33 is modulated during clinical and experimental HTx rejection and free IL-33 is available during early rejection to shape local and systemic immune responses. In addition, that IL-33 remained increased in the grafts of recipients exhibiting less CAV is suggestive of a beneficial role for sustained local IL-33.

Heart transplants lacking IL-33 undergo augmented chronic rejection and increased infiltration by T cells.

To delineate the effect of graft or recipient IL-33 upon heart transplant outcomes in this model of chronic rejection, we completed heterotopic transplantation of *il33*$^{+/+}$ or *il33*$^{-/-}$ Bm12 hearts in *il33*$^{+/+}$ B6 mice and assessed groups of grafts at POD30 and 90-100. A group of *il33*$^{-/-}$ Bm12 hearts transplanted into *il33*$^{+/+}$ B6 mice was also analyzed at POD90. The absence of graft IL-33 resulted in increased graft pathology and immune infiltration at both time points (**Figure 2A-I**). Using computer-aided image analysis of whole slide images of (WSI) of H+E (**Figure 2B**) and Tri-chrome stained samples (**Supplemental Data Figure 2A-B)** we established increased early vascular occlusion in *il33*$^{-/-}$ Bm12 hearts transplanted in either *il33*$^{+/+}$ B6 recipients (**Figure 2A, C**). Both vasculopathy and fibrotic disease were increased at the POD90-100 timepoint in *il33*$^{-/-}$ Bm12

hearts transplanted in either *il33*$^{+/+}$ *or il33*$^{-/-}$ B6 recipients (**Figure 2B-D**). Graft survival reflected the above observations of increased pathology and immune infiltrate, as the absence of graft IL-33 resulted in the accelerated loss of Bm12 heart graft function (**Figure 2E**). While *il33*$^{+/+}$ Bm12 grafts exhibited long-term functioning as expected (40, 41), *il33*$^{-/-}$ Bm12 grafts instead showed late rejection (median survival time=57.5).

We also used immunohistochemistry for CD3, CD11b, and Foxp3 to characterize the immune infiltrate present at these time points. These assessments revealed that the absence of local IL-33 resulted in increased CD3^{+} and Foxp3^{+} cell infiltrate but did not alter the frequency of CD11b^{+} cells (**Figure 2F-I and Supplemental Data Figure 2C-E**). While previous studies have suggested that IL-33 is important for Treg accumulation in injured skeletal muscle (31), graft IL-33 did not appear to modulate local Treg frequency, as their numbers were increased in *il33*$^{-/-}$ Bm12 relative to *il33*$^{+/+}$ Bm12 and appeared to be part of an overall increase in CD3^{+} cells in the absence of IL-33 (**Figure 2F-H and Supplemental Data Figure 2C-E**).

Although there was the emergence of limited recipient IL-33^{+} cells in the graft by POD90-100, these cells appeared to have minimal functional impact as there was no significant alteration seen in the level of immune infiltration or vascular occlusion between *il33*$^{-/-}$ Bm12 grafts in *il33*$^{+/+}$ *or il33*$^{-/-}$ B6 recipients (**Figure 2B-G**). There was a slight decrease in fibrotic area observed when both the graft and recipient lacked IL-33, suggesting a potential pro-fibrotic role for recipient IL-33 (**Figure 2D).** In total, these data provided evidence that graft-derived IL-33 acts as a regulatory alarmin that limits chronic rejection.

Graft IL-33 does not alter systemic immune responses after heart transplantation.

We next assessed if the lack of IL-33 in the graft impacted splenic lymphoid cells at POD3, 30, and 90-100 by flow cytometry. Analysis at the early timepoint did not uncover any global differences in the frequencies of CD3^{+} T cells, B cell, or CD11b^{+} myeloid cells between spleen of WT B6 recipients of *il33*$^{-/-}$ or *il33*$^{+/+}$ Bm12 heart grafts at POD3 *(***Supplemental Data Figure 3A-**

B*).* Nor were there differences in the frequency of naïve ($CD44^-$ $CD69^-$ $CD62L^+$ $KLRG1^-$) $CD4^+$ T cells or $CD4^+$ T effector ($CD44^+$ $CD69^+$ $CCR7^-$ $KLRG1^-$) between WT B6 recipients of *il33*$^{-/-}$ or *il33*$^{+/+}$ Bm12 heart grafts at POD30 (*data not shown*). Flow analyses of WT B6 recipient spleen cells at POD90-100 revealed the anticipated (41) increase in $CD4^+$ T effector memory ($CD4^+$ $CCR7^{lo}$ $CD44^+$) cells (**Supplemental Data Figure 4A-B**) was similar between recipients WT B6 recipients of *il33*$^{-/-}$ or *il33*$^{+/+}$ Bm12 heart grafts. Thus, the increased graft pathology observed in *il33*$^{-/-}$ Bm12 transplants at either POD30 or POD90-100 did not appear to be associated with significant differences in systemic recipient $CD4^+$ T cell response to H2-Ab1^{Bm12}.

While chronic rejection-associated fibrosis and vasculopathy of Bm12 allografts takes place in the presence of $CD4^+$ $Foxp3^+$ Treg, an increase in the presence and the suppressive function of Treg is important for the long-term survival of Bm12 heart transplants (40). However, in spite of ample evidence that delivery of rIL-33 produces systemic increases in Treg that protected cardiac allografts (29, 45), the absence of IL-33 in the allograft did not impact the early presence of $ST2^+$ or $ST2^-$ Treg in the spleen at POD3 (**Supplemental Data Figure 3A-B**). We also observed the expected systemic increases in $Foxp3^+$ Treg, including the $ST2^+$ subset, at POD30 and 90-10 post-transplant of both *il33*$^{-/-}$ and *il33*$^{+/+}$ Bm12 grafts (**Supplemental Data Figure 4C-F**).

Local IL-33$^+$ *regulates pro-inflammatory myeloid cells in the graft cells early after heart transplantation.*

The heart transplant data to this point indicate that IL-33 is limiting intra-graft $CD3^+$ cells and early vasculopathy, but not shaping systemic $CD4^+$ T cell responses, to temper chronic allograft rejection. The importance of trafficking donor and recipient myeloid cells to the secondary lymphoid tissues where they prime alloreactive T cell, which then leave to attack the graft, is appreciated (46, 47). In addition to acting as dominant drivers of local pro-inflammatory responses and tissue injury after cardiac IRI (48, 49), data have emerged that recruited myeloid cells are

also critical for sustaining early T cell responses in the allografts (14, 47). Guided by these data, we examined if graft derived IL-33 was influencing graft or systemic myeloid cells responses after cardiac transplantation. While graft (**Figure 2I and Supplemental Data Figures 2E and 3C-D**) and spleen global myeloid cell populations (**Supplemental Data Figures 3A-B and 5A-D**) were not quantitatively impacted by an absence of graft IL-33, the comparison of *il33*$^{+/+}$ and *il33*$^{-/-}$ Bm12 transplanted into *il33*$^{+/+}$ B6 recipients by flow cytometry at POD3 revealed profound early qualitative differences in graft myeloid cells (**Figure 3**). It is understood that by three days post-transplant, recipient monocytes infiltrate heart or kidney transplants and transition to monoDC (CD11b^{+}CD11c^{+}MHCII^{+}) that mediate allograft rejection by promoting the proliferation and survival of CD3^{+} T cells in the graft (14). Recipient monocytes also differentiate into CD11b^{+}F4/80^{+}Ly6C^{hi} and Ly6C^{lo} macrophages at early timepoints post-heart transplantation to shape graft pathology and alloimmunity (16). Comparing CD11b^{+} populations from *il33*$^{-/-}$ Bm12 to *il33*$^{+/+}$ Bm12 at POD 3, revealed that in the absence of IL-33, Bm12 grafts had a slight increase in CD11c^{+} monoDCs (CD11b^{+}CD11c^{+}MHCII^{+}; **Figure 3A-B**). More profound, however, was the increase in pro-inflammatory Ly6C^{hi} macrophages (CD11b^{+}CD11c^{-}F4/80^{+}Ly6C^{hi}; **Figure 3C-D**), including an MHCII^{hi} subset (**Figure 3C-D**). Inducible nitric oxide synthase (iNOS) is both a phenotypic marker of pro-inflammatory macrophages and an effector molecule that enables their functions (50, 51). The early increases in inflammatory macrophages persisted in *il33*$^{-/-}$ Bm12 grafts as immunofluorescent staining of POD30 grafts uncovered an increased frequency of iNOS^{+}CD11b^{+} cells in those lacking IL-33 (**Figure 3E-F**).

Recipient CCR2^{+} monocyte-derived cells are the mediators of augmented vasculopathy in IL-33 deficient heart grafts.

The C-C chemokine receptor type 2 (CCR2) is critical for monocyte tissue entry (52) and subsequent CCR2^{+} monocyte-derived macrophage differentiation into Ly6C^{hi} pro-inflammatory macrophages that promote tissue damage and contribute to allograft rejection (16, 53). To

establish if the increased pro-inflammatory macrophages observed in the absence of graft IL-33 were propagating accelerated chronic rejection, we assessed B6 WT and *Ccr2*$^{-/-}$ recipients of *il33*$^{+/+}$ BM12 heart transplants at POD30. IL-33-deficient Bm12 grafts again exhibited a significant increase in vascular occlusion typical of this timepoint in WT mice (**Figure 2C**), however, IL-33-deficient allografts in *Ccr2*$^{-/-}$ recipients were protected against this accelerated vasculopathy (**Figure 3G-F**). In total, our findings to this point establish that graft IL-33 is important to limit early allograft vasculopathy by negatively regulating the generation of pro-inflammatory macrophages from CCR2^{+} recipient cells.

Restoring local IL-33 reduces graft inflammatory myeloid cells and prevents chronic rejection.

We have recently revealed that matrix bound nanovesicles (MBV) embedded within the ECM contain bioactive IL-33 (27) and we next assessed if restoring IL-33 locally using MBV could reverse the increase in local inflammatory cells or prevent accelerated chronic rejection. We generated a pliable hydrogel containing IL-33-compentent (IL-33^{+}) or IL-33-deficient (IL-33^{-}) MBV and adhered them to grafts immediately after transplantation. Hydrogels containing IL-33^{+} MBV, but not IL-33^{-} MBV, prevented the loss of IL-33-deficient grafts to the accelerated chronic rejection observed before (**Figure 4A**). Consistent with an anti-inflammatory role for local IL-33, we found that IL-33^{+} MBV delivery reduced the number of pro-inflammatory Ly6C^{hi}F4/80^{+} macrophages, but not CD11b^{+}11c^{+} monoDC in the grafts at POD3 (**Figure 4B-C** and **Supplemental Data Figure 6**). IL-33^{+} MBV administration at the transplant site did not significantly alter either population in the spleen at this timepoint (**Figure 4D-E** and **Supplemental Data Figure 6**), suggesting that the dominant effect of IL-33 was local. Using hydrogel-based delivery of IL-33 to correct the deficit of graft IL-33 in *il33*$^{-/-}$ Bm12 grafts, we confirmed that local IL-33 functions to limit the generation of inflammatory macrophages in the allograft early after transplantation. These data also suggest that delivery of regulatory biomolecules, such as IL-33, locally to the graft using MBV and hydrogels is feasible and promising for chronic rejection prophylaxis.

IL-33-stimulation poises macrophages through metabolic reprogramming for a regulatory and reparative response.

Metabolic remodeling of macrophages is critical to support the energy and metabolite demands required for their response to environmental input during infections and after injury (54, 55). Our above data led us to hypothesize that IL-33 may act like IL-4 and IL-10 to augment FA uptake and oxidative phosphorylation (OXPHOS) which supports the function of regulatory and reparative macrophages (56, 57) and tolerogenic DC (58). To characterize the precise metabolic changes induced by IL-33, we compared the metabolic impact of IL-33 on bone marrow-derived macrophages (BMDM) to that of the well-characterized BMDM responses to IL-4 or LPS/IFNγ stimulation (50, 51). It was clear that IL-33 behaved similarly to IL-4 and augmented OXPHOS to augment Basal Respiration and ATP production (**Figure 5A-B**). This effect was in direct contrast to LPS/IFNγ stimulation, which reduced these measures as metabolic activity shifted towards glycolysis (**Figure 5A-B**). Global metabolite assessment indicated that IL-33, like IL-4, augmented macrophage ATP generation via OXPHOS using an intact TCA cycle. Both IL-4- and IL-33-stimulated macrophages displayed increased concentrations of carnitine (**Supplemental Data Figure 7A)**, which is required for FA transport into the mitochondria (55). IL-4 and IL-33 also increased concentrations α–ketoglutarate (AKG) and glutamate (**Supplemental Data Figure 7B).** There was no evidence in IL-33-activated BMDM for increased glucose-6-phosphate (G6P; **Figure 5C**), the first intermediate of glycolysis, or a buildup of lactate (**Figure 5C**), that occurs as macrophages use glucose to generate limited ATP using anaerobic glycolysis (55). This was in contrast to LPS/IFNγ-activated BMDM that had high concentrations of NO (**Supplemental Data Figure 7D-E)**, G6P and lactate (**Figure 5C**). LPS/IFNγ-activated BMDM also displayed the expected (36, 37, 51) increase in succinate, citrate, and itaconate due to a NO-induced disruption of the TCA cycle caused by inhibition of isocitrate dehydrogenase (IDH) (**Figure 5C)**. IL-33-

stimulated macrophage were metabolically distinct from IL-4-stimulated macrophages in that they did not display glutamine consumption or accumulate the amino acid ornithine (**Supplemental Data Figure 7C**) (50). Instead, IL-33-stimulated macrophages exhibited high levels of aspartate, malate, fumarate, and increased concentration of arginine relative to both LPS/IFNγ- or IL-4-stimulated macrophages (**Supplemental Data Figure 7A**). These metabolites are components of the aspartate-arginosuccinate shunt (AASS), which connects the TCA cycle with the generation of effector metabolites, such as ornithine and citrulline/NO (50, 59, 60).

CD301 is often used as a marker of IL-4- or "alternative" macrophage activation and this subset of macrophages is critical for wound repair (61). IL-33-stimulation increased CD301 expression on BMDM, albeit to a lesser extent relative to IL-4 (**Figure 5D-E**). When FA uptake was blocked, a profound inhibition of IL-33-induced CD301 expression resulted (**Figure 5D-E**). While the role for FA uptake and oxidation in macrophage polarization remains controversial (62), our data are consistent with prior studies showing that disruption of FA uptake through inhibitors or loss of the FA translocase CD36 in mice and humans limits the generation and function of immunosuppressive and regulatory myeloid cells (56, 63). Thus, IL-33-stimulated macrophages reflect a unique macrophage that is "poised" through metabolic reprogramming for a regulatory and reparative response typical of IL-4-activated macrophages, while primed for potential effector responses through an active AASS (See Schematic Summary in **Supplemental Data Figure 7F**).

IL-33 limits pro-inflammatory signal induced iNOS expression

Early transplantation-associated IRI and alloimmune-mediated damage of the heart will release IL-33, TLR4-ligands, and pro-inflammatory cytokines together. Global metabolomic analysis of how IL-33 impacted BMDM receiving simultaneous LPS/IFNγ-stimulation revealed that IL-33 did not modulate aerobic glycolysis, as G6P generation was sustained (**Figure 5C**). However, we observed reduced lactate concentrations suggesting limited anaerobic glycolysis, as well as decreased levels of citrate and succinate (**Figure 5C**). Citrulline, which is produced

with NO by iNOS from arginine was also reduced in LPS/IFNγ-stimulated BMDM by the co-presence of IL-33 (**Figure 5C**). NO is critical to macrophage metabolic reprogramming as it disrupts the electron transport chain by targeting Complex I and IV and decreases IDH (51, 64). Decreased IDH activity results in itaconate inhibition of succinate dehydrogenase (SDH), which causes succinate to reach levels triggering pro-inflammatory activities (37). These past studies, combined with the observed increased in $iNOS^{+}CD11b^{+}$ cells in *il33*$^{-/-}$ Bm12 grafts (**Figure 3E-F**), led us to ask if IL-33 signaling controlled macrophage induction of iNOS. Splenic macrophages receiving simultaneous stimulation with IL-33 and LPS/IFNγ (**Figure 5F**) or receiving IL-33 stimulation first, followed by LPS/IFNγ-stimulation (**Figure 5G**) had decreased induction of *Nos2*. BMDM stimulated with IL-33 and LPS/IFNγ also exhibited a profound reduction in iNOS protein (**Figure 5H**). These data are consistent with the capacity of IL-33 to limit the expression of $iNOS^{+}$ in macrophage and prevent metabolic reprogramming supporting pro-inflammatory functions.

Graft IL-33 targets infiltrating macrophages to stimulate FA uptake and limits macrophage differentiation into an iNOS^{+} *pro-inflammatory subset causing rejection.*

FA uptake reduces the stimulatory function of tumor-associated DC and supports the immunosuppressive mechanisms of myeloid-derived suppressor cells (63, 65). Likewise, FA uptake contributes to the generation of alternatively activated, M2 macrophages that are critical to cardiac tissue repair after ischemia (56, 66). IL-33 poised BMDM for differentiation towards a M2-like state through FA uptake while limiting the induction of iNOS, which is necessary for a metabolic and pro-inflammatory shift in macrophages towards glycolysis. By comparing $CD11b^{+}$ populations from *il33*$^{-/-}$ Bm12 to *il33*$^{+/+}$ Bm12 heart transplants at POD3, we also revealed a significant reduction in levels of FA uptake in the absence of IL-33 in $CD11b^{+}CD11c^{-}F4/80^{+}Ly6C^{hi}$ macrophages (**Figure 6A-B**). The $Ly6C^{lo}$ macrophage subset displayed a similar trend towards

decreased FA uptake (**Figure 6A-B**). These data supported an important role for graft IL-33 in stimulating FA uptake in recipient myeloid cells infiltrating the graft.

Other immune cells, particularly Treg (29-31, 67-69), express ST2 and could respond to IL-33 and control myeloid cell activation to improve transplant outcomes. We used B6 *LysM*^{Cre}x*St2*$^{fl/fl}$ mice, which have targeted deletion of ST2 on F4/80^{+} macrophages, but not Treg or other immune cells (**Supplemental Data Figure 8**), as *il33*$^{+/+}$ Bm12 heart graft recipients to address this. Using this precise model, we confirmed that IL-33-signaling to macrophages at early timepoints post-transplant limits the differentiation of graft infiltrating myeloid cell into pro-inflammatory iNOS^{+}CD206^{lo} macrophages (P1; **Figure. 6C-E**), but not CD11c^{+}MHCII^{hi} monoDC or CD206^{hi} macrophages (P2; **Figure 6C-E**).

The absence of IL-33-signalling in iNOS^{+}CD206^{lo} macrophages also resulted in augmented levels of iNOS in these cells (P1; **Figure. 6E)** and decreased FA uptake in this macrophage subset **(P1; Figure 6F).** The deletion of ST2 from recipient macrophages did not, however, alter Treg in the graft or spleen (**Supplemental Data Figure 9**). This loss of IL-33 signaling to macrophages, like the absence of graft IL-33 (**Figure 2E**), resulted in accelerated rejection of *il33*$^{+/+}$ Bm12 grafts (**Figure 6G**). In total, these data establish that IL-33 directly targets macrophages to induce a metabolic program supporting FA uptake and regulating iNOS induction that limits the generation of pro-inflammatory macrophages causing accelerated graft loss.

DISCUSSION

Myeloid cells are a dominant component of the infiltrating immune cells during acute rejection (70) and that increased macrophage numbers present in renal allografts correlates with chronic rejection and poor outcomes (71). Increased graft and circulating myeloid cells are common in samples from recipients with acutely- and chronically-rejected heart (72, 73) grafts. Yet only recently have the precise mechanisms by which graft infiltrating myeloid cells contribute to rejection started to crystalize. Recipient monocytes rapidly infiltrate ischemic allografts and differentiate into monoDC and macrophage subsets that then support the local alloreactive T cell response (14, 16, 17). Intracellular alarmins including HMGB1, IL-1α, nuclear DNA, mitochondrial DNA, as well as ECM components like hyaluronan and heparin sulfate are released upon tissue injury from IRI or alloresponses that then trigger TLRs on myeloid cells to direct their differentiation and stimulate the type 1 immunity mediating acute and chronic rejection. Recent animal studies have established that graft infiltrating monocyte recognizing allogenic molecules, such as the polymorphic signal regulatory protein α (SIRPα), mature into monoDCs that expressed IL-12 and stimulated T cell proliferation in the graft (74). Pro-inflammatory functions of myeloid cells involve reprogramming of their cellular metabolism towards reliance on glycolysis to support their inflammatory functions (54, 75). Our data make a convincing case that IL-33 is unique among alarmins and functions as a “regulatory” alarmin after transplantation to targets infiltrating myeloid cells and temper pro-inflammatory responses by supporting cellular metabolism that enables homeostatic or tissue protective functions (75, 76).

Cardiac tissue has limited capacity for repair and cardiomyocytes lost to IRI and alloimmune responses will be replaced by fibrotic scar tissue that prevents cardiac rupture but limits function (77). Thus, methods to limit damage and cardiomyocyte loss after heart transplant are attractive therapeutics. Shortly after cardiac IRI, an early pro-inflammatory period takes place involving Ly6C^{hi} monocytes and inflammatory macrophages that clear debris by proteolysis and

phagocytosis and promote local inflammation through secretion of IL-1β, IL-6, IL-12 family members and TNFα (78-80). This initial pro-inflammatory period typically peaks after 3-4 days and initiates a period of resolution and remodeling supported by TGFβ, IL-10 and involves $Ly6C^{lo}$ monocytes and alternatively-activated macrophages (48, 80). Dysregulation of this process or domination by the pro-inflammatory period translates into increased pathological remodeling and fibrosis (80). Our characterization of the graft myeloid compartment at 3 days post-transplant revealed that the IL-33 restricts the pro-inflammatory capacity of graft-infiltrating, recipient monocyte-derived macrophages that cause chronic rejection-associated vasculopathy and accelerated graft loss. The restoration of local IL-33 limited $Ly6C^{hi}$ macrophages and reduced chronic heart rejection of *il33*$^{-/-}$ Bm12 grafts. These observations are similar to those when anti-HMGB1 antibodies are delivered after Bm12 heart transplant into B6 recipients. In these studies, targeting HMGB1 reduced the presence of intragraft $CD11b^{+}F4/80^{+}$ macrophages, $CD11c^{+}$ monoDC, and T cells expressing IFNγ and IL-17A to decrease fibrosis and vessel disease at day 28 post transplantation (20). Based on these considerations, we conclude that a dominant early protective function of IL-33 after heart transplantation is to limit the pro-inflammatory capacity of local myeloid cells early after heart injury.

Myeloid cells need to be plastic and respond to local stimuli to support host defenses against infections, but also then contribute to the immune regulation and restoration of tissue function. The importance of modulation of macrophage metabolism to carry out these activities has come to light recently (54) and our current studies provide insights into the way that the alarmin IL-33 contributes to regulation of macrophage in the tissues after transplantation. IL-33 stimulation of macrophages augmented OXPHOS and FA uptake, both of which support reparative and regulatory myeloid cell functions. While IL-33 was not as potent effector of alternative macrophage activation as IL-4, FA uptake was important for both to increase phenotypic markers of alternative activation.

We have shown previously that IL-33 activates NF-κB and p38 in macrophages (27) and monoDC, which facilitate their ability to expand Th2 cells and Treg secreting IL-5, IL-10, and IL-13 (30, 69, 81). These cytokines act on macrophages and other cells in the adipose to maintain systemic metabolic homeostasis (82, 83). Dahlgren et al has recently established that Treg and $ST2^+$ cDC2 exist with ILC2s around larger vessels in tissues under homeostatic conditions and IL-33^+ stromal cells (ASC) are crucial to maintain these homeostatic niches (42). Our current observations extend these data and establish that IL-33 may function as part of a homeostasis maintenance or restoration system in the transplant microenvironment. Specifically, in the absence of IL-33 an uncontrolled early inflammatory response involving increased inflammatory macrophages leads to greatly augmented chronic rejection. Our mechanistic studies showed that IL-33 acts similar to IL-4 and IL-13 and increases mitochondrial function and FA uptake (56). This is in contrast to TLR4 ligands, like HMGB1 or LPS, which stimulate TLR4 to drive glycolysis and epigenetic modifications enabling inflammatory cytokine production (16). Both ST2 and TLR4 are IL1R/TLR superfamily members that rely on MyD88 as a signaling adaptor and use NF-κB and p38 as downstream effector signaling molecules (26). Both receptors activate mammalian target of rapamycin (mTOR) (16). Despite the similarities, however, there are nuanced differences in signaling between TLR4 and ST2 that produce the contrasting functions observed when these closely related pathways are stimulated. One clear difference we identified was the capacity of IL-33 to limit the induction of iNOS in macrophages *in vitro* and *in vivo*. Regulation of iNOS is important, as it prevents the NO-induced metabolic reprogramming that enables pro-inflammatory macrophage functions (51, 64). IL-33-exposed myeloid cells can utilize OXPHOS, where TLR4-stimulated cells will be locked into a metabolic program relying on glycolysis and associated with pro-inflammatory activities (54). The pharmacological inhibition of glycolysis prevents DC transition from immature, steady state DC to immunogenic DC (84) and delivery of nanoimmunotherapeutics to macrophage in the allograft and preventing HMGB1-induced

glycolysis supports allograft acceptance when delivered with co-stimulatory blockade (16). Thus, IL-33 represents an endogenous regulatory molecule able to trigger a pathway promoting myeloid cell metabolism towards one supporting injury repair functions and allowing reestablishment of local homeostasis.

Several populations of immune cells that can shape transplant outcomes express ST2 and respond to IL-33. These including macrophages (27), DC (30, 42, 81), $CD8^+$ (85), $CD4^+$ T cells (86), and Treg (29-31, 67-69). Previously our work, and that of others, revealed that delivery of rIL-33 promoted cardiac allograft survival by expanding naturally-occurring Treg, including an $ST2^+$ subset, that limited systemic Type 1 responses (29). Since then, the secretion of the epidermal growth factor amphiregulin (Areg) by IL-33-stimulated $ST2^+$ Treg has been shown to support tissue repair after injury to the skeletal muscle and lung epithelium (31, 67, 68). IL-33 also induces Treg and ILC2 secretion of IL-10 and IL-13 in the adipose tissues and injured lung to limit local inflammation and generate M2-macrophages implicated in tissue repair and homeostasis (69, 82, 83). ST2 is also expressed by stromal cells and IL-33 has been suggested to be directly protective for cardiac myocytes (87). An important finding from this study was the demonstration that IL-33 from the graft directly targets recipient-derived macrophages to limit their differentiation into a detrimental pro-inflammatory subset that causes graft loss. These data identify an important protective role for IL-33 and exciting future studies relying on further immune cell and tissue specific disruption of ST2 will help us understand how IL-33 coordinates immune and stromal response to injury after heart transplantation.

Our rodent data suggest that IL-33 levels in the graft increase rapidly but decrease during the post-transplant period. Our examinations of clinical transplant specimens reveal that IL-33 remained increased in grafts exhibiting less vasculopathy and this is suggestive of a beneficial role for sustained local IL-33 that would parallel the protective function revealed for IL-33 in our rodent chronic rejection model. These data are similar to studies by the Mathis group that show that IL-33 expression spikes early after skeletal injury in young mice, but not old mice which have

lost IL-33 expressing cells (31). Like our studies in which grafts lacking IL-33 suffer increased chronic rejection, in aging mice poor repair of skeletal muscle was associated with a loss of IL-33 expressing cells (31). Cardiac allografts from older donors have increased risk of chronic rejection (88) and it will be important to define if age related loss of IL-33 may contribute to this risk. We have found that IL-33 is contained in MBV of the ECM of various tissues, including cardiac (27). During the development of cardiac fibrosis the ECM is extensively remodeled (89). If this remodeling involves modulation of IL-33 in the ECM to influence the function of local $ST2^+$ immune cells will also be a significant question to answer. If $IL\text{-}33^+$ cells are indeed reduced in aged donors or if local IL-33 concentrations are depleted during pathological fibrotic remodeling, then our data, showing that local IL-33 delivery reduced the chronic rejection of IL-33-deficient hearts, suggest this type of therapy may be a highly effective CR prophylactic.

The revealed biological impacts of IL-33 on macrophages and heart transplantation outcome were profound and our data support the development of targeted $IL\text{-}33^+$ therapy to prevent chronic rejection. The concept to stimulate natural reparative pathways is novel relative to other approaches in the DAMP/alarmin space, which instead aim to prevent or block TLR signaling. One advantage of augmenting reparative pathways is that, unlike TLR antagonists or immunosuppressant molecules, this would not stand in the way of normal pathogen responses (18). In addition to heart transplants, other commonly transplanted solid organs, including kidney (90), liver (91), and lung (92), as well as vascular composite allografts (93), all suffer from immunosuppressant-resistant chronic rejection-associated fibrosis and vasculopathy. It will be important to determine if endogenous or delivered IL-33 also acts as a regulatory alarmin in these transplant microenvironments to limit myeloid cell differentiation.

METHODS

Clinical Specimens.

Pediatric heart transplant recipient samples were obtained from a prospective study completed at the Children's Hospital of Pittsburgh of UPMC described previously (94) or an NIAID-funded study entitled, "An Observational Cohort Study to Determine the Impact of Alloantibodies and Antibodies to Self-Antigens on Chronic Allograft Function up to 5 years after Pediatric Heart Transplantation". This study enrolled recipients from 9 pediatric heart centers in the U.S. and Canada. Patients received thymoglobulin induction therapy with subsequent tacrolimus-based immunosuppression plus adjunctive sirolimus or mycophenolate mofetil and underwent serial post-HTx allograft surveillance EMB at 1-2 weeks, 2-4 weeks, 2 months, 4 months, 6-7 months, 10-12 months, and then annually thereafter until the first of either the 5-year post-transplant study visit, study withdrawal, of end of study follow-up. Patients also underwent EMB if rejection was suspected and to assess resolution following the rejection treatment. Coronary angiograms were obtained at 12 months post-transplant and annually thereafter and were analyzed by a single blinded pediatric cardiologist at the study core angiography laboratory at Washington University at St. Louis. Analyzed serum were identified and assessed for IL-33 at times of pathologist-diagnosed acute cellular rejection (ACR) or antibody-mediated rejection (AMR) happening within the first 21-50 days after transplant (n=11 samples from 10 subjects) or suffering mild (n=16 samples from 10 subjects) or severe (n=12 samples from 5 subjects) chronic rejection-associated coronary artery vasculopathy at least 300 days post-transplant. Serum from the Starzl Biorepository for normal healthy non-transplanted adults (n=8) was also assessed. We also separately identified and compared EMB samples from ACR events (n=7 in 4 subjects), AMR events (n=7 in 5 subjects), and no rejection events (n=7 in 6 subjects) in the first-year post transplant using immunostaining for IL-33. Multiple EMB from pediatric heart transplant recipients suffering severe (n=8 in 3 subjects) versus mild CAV (n=12 in 3 subjects) after the first year were also assessed.

Animals.

B6, Bm12, *LysM*^{Cre}, and *Ccr2*$^{-/-}$ mice were purchased from Jackson Laboratories. The *il33*$^{-/-}$ mice were from S. Nakae (University of Tokyo, Tokyo, Japan) (38). Bm12 *il33*$^{-/-}$ mice were generated by 6 times backcrossing Bm12 mice on to the *il33*$^{-/-}$ background at the University of Pittsburgh. *St2*$^{-/-}$ mice were originally generated on a BALB/c background (95) and backcrossed 10 times onto the B6 before use. The B6 *St2*$^{flox(fl)}$ mice were provided by Dr. Giorgio Trinchieri (National Cancer Institute, Bethesda, Maryland) and crossed to *LysM*^{Cre} to generate *LysM*^{Cre}x*St2*$^{fl/fl}$ mice. All animals were housed in a specific pathogen-free facility maintained by the University of Pittsburgh.

Vascularized heart transplantation.

Donor hearts were transplanted into recipients through end-to-side anastomosis of the donor ascending aorta and pulmonary artery to recipient abdominal aorta and inferior vena cava as described (14). In some experiments, MBV isolated from decellularized IL-33^{+} mouse intestines as described (96) were diluted in a porcine urinary bladder matrix hydrogel to final concentration of 1 mg/ml MBV. Graft were covered in hydrogel containing 40 μg diluted MBV after reperfusion of the graft. The gut was replaced and allowed to resume its normal position around the grafted heart while the MBV in hydrogel stably adhere the heart surface. Graft function was verified daily by abdominal palpation of heart contractions until indicated day of harvest.

Isolation of splenic, peritoneal, and graft-infiltrating leukocytes.

Mice were anaesthetized and perfused with PBS+0.5% heparin via the left ventricle until the fluid exiting the right ventricle did not contain visible blood. Hearts or heart grafts were removed, cut into fragments, and homogenized in a Gentle MACS C tube in media containing 350U/ml type IV collagenase (Gibco) and 20 μg/ml DNAse I (Sigma) using program E on a

gentleMACS dissociator (Miltenyi Biotec). Single-cell suspensions were then obtained through filtration using a 40 μm cell strainer and centrifuged over a Lympholyte-M (Cedarlane) density gradient. Spleens from recipient or naïve mice were isolated and single cell suspensions generated following mechanical dissociation and RBC lysis. Isolation of splenic macrophages was completed using positive selection with Anti-F4/80 MicroBeads (Miltenyi Biotec). Peritoneal cells were obtained by flushing the peritoneal cavity with 1 ml of cold PBS.

Generation of bone marrow-derived macrophages (BMDM).

Murine BMDM were generated similar to described (50, 51, 96). Briefly, BM was harvested, washed, and plated in complete medium at 1×10^6 cells/mL. Cells were allowed to differentiate into macrophages for 7 days in the presence of macrophage colony-stimulating factor (MCSF) (20 ng/ml, Biolegend) or 10% L929 cell supernatant containing MCSF, with complete media changes every 48 h. On day 7, macrophages were cultured for 15-18 h at 37°C and 5% CO_2 in complete media alone (M0) or media supplemented with one or combinations of the following: 1) 20 ng/mL IFNγ (Affymetrix eBioscience) and 100 ng/mL LPS (Sigma Aldrich); 2) 20 ng/mL IL-4 (Invitrogen); 3) 20 ng/ml IL-33 (Peprotech). After the incubation cells were washed with sterile PBS and utilized for experimental assays.

Histological and Immunohistochemical staining.

Naïve mouse hearts and heart transplants were formalin-fixed, paraffin-embedded, sectioned (4 μm), adhered on glass slides, and stained with H+E or Masson's Trichrome following standard protocols. Using NearCYTE software (http://www.nearcyte.org) as we have described (94), blue fibrosis$^+$ areas (mm^2) were divided by the whole tissue area (mm^2) and multiplied by 100 to give a percentage fibrotic area measure. Vascular occlusion was calculated using NearCYTE to quantitate the total and open lumen area (mm^2) for each artery. These values were

used to generate a percentage vascular occlusion for each identified artery and a mean % vascular occlusion calculated for each recipient. CD3, CD11b and Foxp3 staining was completed using primary antibodies to CD3 (Abcam, ab1669), CD11b (BD Pharmingen, 550282), Foxp3 (Abcam, ab54501), and then secondary antibodies of biotinylated goat anti-rat (Vector, BA-9400), goat anti-rabbit (Vector, BA-1000), horse anti-goat (Vector, BA-9500). The total number of CD3, Foxp3, or CD11b positive cells was calculated manually for each tissue and divided by the total tissue area calculated by NearCYTE to yield a cells/area (mm^2) measure for each sample.

Quantitative Immunofluorescence.

Optimal cutting temperature compound (Fisher)-embedded frozen mouse HTx or naïve hearts were sectioned (6 μm), placed on glass slides, and stained for CD45 (BD Biosciences, 550539), vimentin (Abcam ab73159), IL-33 (R&D Systems, AF3626) and fluorescent-conjugated and species-specific secondary antibodies following protocols established in the Center for Biologic Imaging, University of Pittsburgh (http://cbi.pitt.edu) as described (29). IL-33 staining of paraffin-embedded EMB sections (4 μm) from pediatric heart transplant recipients was completed following deparaffinization and antigen retrieval similar to methods we have described (94). Intra-graft macrophage multiplex immunolabeling of paraffin-embedded transplant sections (5 μm) for CD11b (Abcam, ab128797) and iNOS (Thermo Fisher, PA3030A) was completed following deparaffinization and antigen retrieval using standard protocols and multistep labeling. Full details can be found in the *Supplemental Methods*.

ELISA.

Recipient serum levels of IL-33 were measured using commercial kits (R&D Systems, DY3625). Samples were isolated at the time of collection, frozen and stored at -80°C until use.

On the day of assessment, samples were batch thawed and determinations of IL-33 completed in triplicate according to manufacturer specifications. Assay limit of detection was 23.44 pg/mL.

Flow Cytometry.

Isolated splenocytes and graft-infiltrating leukocytes were blocked with heat-inactivated goat serum (5%), treated with a Live/Dead distinguishing stain, and labelled with combinations of fluorochrome-conjugated Abs (BD Bioscience, Biolegend, and eBioscience) to distinguish myeloid, T, and B cell populations. Antibodies(Clone #) to CD45.2(104), CD19(1D3), NK1.1(PK136), (CD45R/B220(RA3-6B2), CD49b(DX5), CD90.2(30-H12), Ly6G(1A8); Ly6C (AL-21), CD11b(M1/70), CD11c(HL3); I-A^b(M5/114.15), CD80(16-10A1), CD86(24F), SiglecF(E50-2440), CD301(LOM-14), iNOS(CXNFT), CD206(MR5D3), Gr-1(RB6-8C5), F4/80(BM8), (CD45 (30-F11), CD3(145-2C11), CD4(GK1.5), CD8(53-6.7), CD127(SB/199), CD44(IM7), CCR7(4B12), Foxp3(MF-14), and ST2(DJ8) were utilized. Bodipy^{TM} FL C12 (Invitrogen) was used for FA uptake assessment. Data was acquired with an LSRFortessa (BD Biosciences) or Aurora-10 (Cytek) flow cytometer and analyzed using FlowJo, Version 10.1 (BD Biosciences).

Molecular macrophage assessments.

Cellular mitochondrial bioenergetics, untargeted metabolomic, electron paramagnetic resonance spectroscopy and spin trapping of NO, qRT-PCR, and Western blot analysis of murine BMDM were completed using standard techniques described in the *Supplemental Methods*.

Statistical Analysis.

Statistical analysis was performed using Prism 7 (GraphPad) and statistical tested use indicated in the figure legends. A value of $p<0.05$ was considered statistically significant.

Study approvals.

Rodent breeding and experimental procedures were approved by and performed in accordance with the guidelines of the Institutional Animal Care and Use Committee of the University of Pittsburgh (Protocol #19065158) and complied with the NIH *Guide for the Care and Use of Laboratory Animals*. The clinical study protocol was approved by the IRBs of all participating institutions and written informed consent was obtained from parents/guardians with child assent obtained according to local IRB policy.

Author contributions

ZZ, TFL, QL, GSH, and HRT conceptualized and designed the research. TFL, ZZ, QL, JGB, MV, LRM, GKD, ASR, YCL, HLD, JLD, SJM, MWT, GSH, and HRT performed the experiments. ZZ, TFL, QL, JGB, MV, LRM, GKD, ASR, SS, MHO, JLD, SJM, SGW, MWT, GSH, SCW, AJD, SFB, and HRT analyzed the data and interpreted the results. ZZ, TFL, GKD, MV, LRM, and HRT prepared the figures. TFL, ZZ, MV, GKD, GSH, SFB, and HRT drafted and edited the manuscript.

Acknowledgements

We thank Anna Lucas for technical assistance and animal husbandry support. We thank Ibraheem Khoury, Benjamin Popp, and Drew Lesniak of the STI Research Histology Services for assistance with EMB assessment. This project used the University of Pittsburgh Genomics Research Core RNA Analysis services and Division of Laboratory Animal Resources. This work was supported by numerous NIH grants: R01AR073527(SFB/HRT), R01HL22489(HRT), R56AI139327(HRT), U01AI104336(SAW), R01AI145881(MHO), T32CA082084(GKD), and F30AI147437(GKD). This work benefitted from NIH shared instrumentation grants (S10OD011925 and S10OD023402). ZZ was supported by National Science Foundation of China (81900371) and Natural Science Foundation of Hunan Province (2019JJ50899).

REFERENCES

1. Keogh A. Calcineurin inhibitors in heart transplantation. *J Heart Lung Transplant.* 2004;23(5 Suppl):S202-6.
2. Siu JHY, Surendrakumar V, Richards JA, and Pettigrew GJ. T cell Allorecognition Pathways in Solid Organ Transplantation. *Front Immunol.* 2018;9:2548.
3. Libby P, and Pober JS. Chronic rejection. *Immunity.* 2001;14(4):387-97.
4. Merola J, Jane-Wit DD, and Pober JS. Recent advances in allograft vasculopathy. *Curr Opin Organ Transplant.* 2017;22(1):1-7.
5. Lodhi SA, Lamb KE, and Meier-Kriesche HU. Solid organ allograft survival improvement in the United States: the long-term does not mirror the dramatic short-term success. *American journal of transplantation.* 2011;11(6):1226-35.
6. Zeng Q, Ng YH, Singh T, Jiang K, Sheriff KA, Ippolito R, et al. B cells mediate chronic allograft rejection independently of antibody production. *J Clin Invest.* 2014;124(3):1052-6.
7. Uretsky BF, Murali S, Reddy PS, Rabin B, Lee A, Griffith BP, et al. Development of coronary artery disease in cardiac transplant patients receiving immunosuppressive therapy with cyclosporine and prednisone. *Circulation.* 1987;76(4):827-34.
8. Pollack MS, Ballantyne CM, Payton-Ross C, Cocanougher B, Rowe SK, Grant OJ, et al. HLA match and other immunological parameters in relation to survival, rejection, severity and accelerated coronary artery disease after heart transplant. *Clinical Transplantation.* 1990;4:269-75.
9. Zerbe T, Uretsky B, Kormos R, Armitage J, Wolyn T, Griffith B, et al. Graft atherosclerosis: effects of cellular rejection and human lymphocyte antigen. *J Heart Lung Transplant.* 1992;11(3 Pt 2):S104-10.

10. Raichlin E, Edwards BS, Kremers WK, Clavell AL, Rodeheffer RJ, Frantz RP, et al. Acute cellular rejection and the subsequent development of allograft vasculopathy after cardiac transplantation. *J Heart Lung Transplant.* 2009;28(4):320-7.

11. Uehara S, Chase CM, Cornell LD, Madsen JC, Russell PS, and Colvin RB. Chronic cardiac transplant arteriopathy in mice: relationship of alloantibody, C4d deposition and neointimal fibrosis. *Am J Transplant.* 2007;7(1):57-65.

12. Frank R, Molina MR, Goldberg LR, Wald JW, Kamoun M, and Lal P. Circulating donor-specific anti-human leukocyte antigen antibodies and complement C4d deposition are associated with the development of cardiac allograft vasculopathy. *Am J Clin Pathol.* 2014;142(6):809-15.

13. Zecher D, Li Q, Williams AL, Walters JT, Baddoura FK, Chalasani G, et al. Innate immunity alone is not sufficient for chronic rejection but predisposes healed allografts to T cell-mediated pathology. *Transpl Immunol.* 2012;26(2-3):113-8.

14. Zhuang Q, Liu Q, Divito SJ, Zeng Q, Yatim KM, Hughes AD, et al. Graft-infiltrating host dendritic cells play a key role in organ transplant rejection. *Nat Commun.* 2016;7:12623.

15. Kitchens WH, Chase CM, Uehara S, Cornell LD, Colvin RB, Russell PS, et al. Macrophage depletion suppresses cardiac allograft vasculopathy in mice. *Am J Transplant.* 2007;7(12):2675-82.

16. Braza MS, van Leent MMT, Lameijer M, Sanchez-Gaytan BL, Arts RJW, Pérez-Medina C, et al. Inhibiting Inflammation with Myeloid Cell-Specific Nanobiologics Promotes Organ Transplant Acceptance. *Immunity.* 2018;49(5):819-28.e6.

17. Zhao Y, Chen S, Lan P, Wu C, Dou Y, Xiao X, et al. Macrophage subpopulations and their impact on chronic allograft rejection versus graft acceptance in a mouse heart transplant model. *Am J Transplant.* 2018;18(3):604-16.

18. Todd JL, and Palmer SM. Danger signals in regulating the immune response to solid organ transplantation. *J Clin Invest.* 2017;127(7):2464-72.

19. Yang H, Hreggvidsdottir HS, Palmblad K, Wang H, Ochani M, Li J, et al. A critical cysteine is required for HMGB1 binding to Toll-like receptor 4 and activation of macrophage cytokine release. *Proc Natl Acad Sci U S A.* 2010;107(26):11942-7.

20. Zou H, Yang Y, Gao M, Zhang B, Ming B, Sun Y, et al. HMGB1 is involved in chronic rejection of cardiac allograft via promoting inflammatory-like mDCs. *Am J Transplant.* 2014;14(8):1765-77.

21. Testro AG, Visvanathan K, Skinner N, Markovska V, Crowley P, Angus PW, et al. Acute allograft rejection in human liver transplant recipients is associated with signaling through toll-like receptor 4. *J Gastroenterol Hepatol.* 2011;26(1):155-63.

22. Methe H, Zimmer E, Grimm C, Nabauer M, and Koglin J. Evidence for a role of toll-like receptor 4 in development of chronic allograft rejection after cardiac transplantation. *Transplantation.* 2004;78(9):1324-31.

23. Krüger B, Krick S, Dhillon N, Lerner SM, Ames S, Bromberg JS, et al. Donor Toll-like receptor 4 contributes to ischemia and reperfusion injury following human kidney transplantation. *Proc Natl Acad Sci U S A.* 2009;106(9):3390-5.

24. Terasaki PI, Cecka JM, Gjertson DW, and Takemoto S. High survival rates of kidney transplants from spousal and living unrelated donors. *N Engl J Med.* 1995;333(6):333-6.

25. Matta BM, Reichenbach DK, Blazar BR, and Turnquist HR. Alarmins and Their Receptors as Modulators and Indicators of Alloimmune Responses. *Am J Transplant.* 2017;17(2):320-7.

26. Liew FY, Girard JP, and Turnquist HR. Interleukin-33 in health and disease. *Nat Rev Immunol.* 2016;16(11):676-89.

27. Hussey GS, Dziki JL, Lee YC, Bartolacci JG, Behun M, Turnquist HR, et al. Matrix bound nonovesicle-associated IL-33 activates a pro-remodeling macrophage phenotype via a non-canonical, ST2-independent pathway. *Journal of Immunology and Regenerative Medicine.* 2019;3:26-35.

28. Brunner SM, Schiechl G, Falk W, Schlitt HJ, Geissler EK, and Fichtner-Feigl S. Interleukin-33 prolongs allograft survival during chronic cardiac rejection. *Transpl Int.* 2011;24(10):1027-39.

29. Turnquist HR, Zhao Z, Rosborough BR, Liu Q, Castellaneta A, Isse K, et al. IL-33 Expands Suppressive CD11b+ Gr-1int and Regulatory T Cells, including ST2L+ Foxp3+ Cells, and Mediates Regulatory T Cell-Dependent Promotion of Cardiac Allograft Survival. *Journal of Immunology.* 2011;187(9):4598-610.

30. Matta BM, Lott JM, Mathews LR, Liu Q, Rosborough BR, Blazar BR, et al. IL-33 is an unconventional Alarmin that stimulates IL-2 secretion by dendritic cells to selectively expand IL-33R/ST2+ regulatory T cells. *J Immunol.* 2014;193(8):4010-20.

31. Kuswanto W, Burzyn D, Panduro M, Wang KK, Jang YC, Wagers AJ, et al. Poor Repair of Skeletal Muscle in Aging Mice Reflects a Defect in Local, Interleukin-33-Dependent Accumulation of Regulatory T Cells. *Immunity.* 2016;44(2):355-67.

32. Sanada S, Hakuno D, Higgins LJ, Schreiter ER, McKenzie AN, and Lee RT. IL-33 and ST2 comprise a critical biomechanically induced and cardioprotective signaling system. *J Clin Invest.* 2007;117(6):1538-49.

33. Seki K, Sanada S, Kudinova AY, Steinhauser ML, Handa V, Gannon J, et al. Interleukin-33 prevents apoptosis and improves survival after experimental myocardial infarction through ST2 signaling. *Circ Heart Fail.* 2009;2(6):684-91.

34. Abston ED, Barin JG, Cihakova D, Bucek A, Coronado MJ, Brandt JE, et al. IL-33 independently induces eosinophilic pericarditis and cardiac dilation: ST2 improves cardiac function. *Circ Heart Fail.* 2012;5(3):366-75.

35. Pichery M, Mirey E, Mercier P, Lefrancais E, Dujardin A, Ortega N, et al. Endogenous IL-33 is highly expressed in mouse epithelial barrier tissues, lymphoid organs, brain, embryos, and inflamed tissues: in situ analysis using a novel Il-33-LacZ gene trap reporter strain. *J Immunol.* 2012;188(7):3488-95.

36. Mills EL, Kelly B, Logan A, Costa ASH, Varma M, Bryant CE, et al. Succinate Dehydrogenase Supports Metabolic Repurposing of Mitochondria to Drive Inflammatory Macrophages. *Cell.* 2016;167(2):457-70 e13.

37. Tannahill GM, Curtis AM, Adamik J, Palsson-McDermott EM, McGettrick AF, Goel G, et al. Succinate is an inflammatory signal that induces IL-1beta through HIF-1alpha. *Nature.* 2013;496(7444):238-42.

38. Oboki K, Ohno T, Kajiwara N, Arae K, Morita H, Ishii A, et al. IL-33 is a crucial amplifier of innate rather than acquired immunity. *Proceedings of the National Academy of Sciences.* 2010;107(43):18581-6.

39. McIntyre KR, and Seidman J. Nucleotide sequence of mutant I-Aβbm12 gene is evidence for genetic exchange between mouse immune response genes. *Nature.* 1984;308(5959):551.

40. Schenk S, Kish DD, He C, El-Sawy T, Chiffoleau E, Chen C, et al. Alloreactive T cell responses and acute rejection of single class II MHC-disparate heart allografts are under strict regulation by CD4+ CD25+ T cells. *J Immunol.* 2005;174(6):3741-8.

41. Yuan X, Paez-Cortez J, Schmitt-Knosalla I, D'Addio F, Mfarrej B, Donnarumma M, et al. A novel role of CD4 Th17 cells in mediating cardiac allograft rejection and vasculopathy. *J Exp Med.* 2008;205(13):3133-44.

42. Dahlgren MW, Jones SW, Cautivo KM, Dubinin A, Ortiz-Carpena JF, Farhat S, et al. Adventitial Stromal Cells Define Group 2 Innate Lymphoid Cell Tissue Niches. *Immunity.* 2019.

43. Souders CA, Bowers SL, and Baudino TA. Cardiac fibroblast: the renaissance cell. *Circ Res.* 2009;105(12):1164-76.

44. Kong P, Christia P, and Frangogiannis NG. The pathogenesis of cardiac fibrosis. *Cell Mol Life Sci.* 2014;71(4):549-74.

45. Yin H, Li XY, Jin XB, Zhang BB, Gong Q, Yang H, et al. IL-33 prolongs murine cardiac allograft survival through induction of TH2-type immune deviation. *Transplantation.* 2010;89(10):1189-97.

46. Celli S, Albert ML, and Bousso P. Visualizing the innate and adaptive immune responses underlying allograft rejection by two-photon microscopy. *Nat Med.* 2011;17(6):744-9.

47. Alegre ML, Lakkis FG, and Morelli AE. Antigen Presentation in Transplantation. *Trends Immunol.* 2016;37(12):831-43.

48. Bajpai G, Bredemeyer A, Li W, Zaitsev K, Koenig AL, Lokshina I, et al. Tissue Resident CCR2- and CCR2+ Cardiac Macrophages Differentially Orchestrate Monocyte Recruitment and Fate Specification Following Myocardial Injury. *Circ Res.* 2019;124(2):263-78.

49. Lavine KJ, Epelman S, Uchida K, Weber KJ, Nichols CG, Schilling JD, et al. Distinct macrophage lineages contribute to disparate patterns of cardiac recovery and remodeling in the neonatal and adult heart. *Proc Natl Acad Sci U S A.* 2014;111(45):16029-34.

50. Jha AK, Huang SC, Sergushichev A, Lampropoulou V, Ivanova Y, Loginicheva E, et al. Network integration of parallel metabolic and transcriptional data reveals metabolic modules that regulate macrophage polarization. *Immunity.* 2015;42(3):419-30.

51. Bailey JD, Diotallevi M, Nicol T, McNeill E, Shaw A, Chuaiphichai S, et al. Nitric Oxide Modulates Metabolic Remodeling in Inflammatory Macrophages through TCA Cycle Regulation and Itaconate Accumulation. *Cell Rep.* 2019;28(1):218-30 e7.

52. Lim JK, Obara CJ, Rivollier A, Pletnev AG, Kelsall BL, and Murphy PM. Chemokine receptor Ccr2 is critical for monocyte accumulation and survival in West Nile virus encephalitis. *J Immunol.* 2011;186(1):471-8.

53. Conde P, Rodriguez M, van der Touw W, Jimenez A, Burns M, Miller J, et al. DC-SIGN(+) Macrophages Control the Induction of Transplantation Tolerance. *Immunity.* 2015;42(6):1143-58.

54. O'Neill LA, and Pearce EJ. Immunometabolism governs dendritic cell and macrophage function. *J Exp Med.* 2016;213(1):15-23.

55. Diskin C, and Palsson-McDermott EM. Metabolic Modulation in Macrophage Effector Function. *Front Immunol.* 2018;9:270.

56. Huang SC, Everts B, Ivanova Y, O'Sullivan D, Nascimento M, Smith AM, et al. Cell-intrinsic lysosomal lipolysis is essential for alternative activation of macrophages. *Nat Immunol.* 2014;15(9):846-55.

57. Ip WKE, Hoshi N, Shouval DS, Snapper S, and Medzhitov R. Anti-inflammatory effect of IL-10 mediated by metabolic reprogramming of macrophages. *Science.* 2017;356(6337):513-9.

58. Malinarich F, Duan K, Hamid RA, Bijin A, Lin WX, Poidinger M, et al. High mitochondrial respiration and glycolytic capacity represent a metabolic phenotype of human tolerogenic dendritic cells. *J Immunol.* 2015;194(11):5174-86.

59. Mills EL, and O'Neill LA. Reprogramming mitochondrial metabolism in macrophages as an anti-inflammatory signal. *Eur J Immunol.* 2016;46(1):13-21.

60. Rodriguez PC, Ochoa AC, and Al-Khami AA. Arginine Metabolism in Myeloid Cells Shapes Innate and Adaptive Immunity. *Front Immunol.* 2017;8:93.

61. Shook B, Xiao E, Kumamoto Y, Iwasaki A, and Horsley V. CD301b+ Macrophages Are Essential for Effective Skin Wound Healing. *J Invest Dermatol.* 2016;136(9):1885-91.

62. Nomura M, Liu J, Rovira, II, Gonzalez-Hurtado E, Lee J, Wolfgang MJ, et al. Fatty acid oxidation in macrophage polarization. *Nat Immunol.* 2016;17(3):216-7.

63. Al-Khami AA, Zheng L, Del Valle L, Hossain F, Wyczechowska D, Zabaleta J, et al. Exogenous lipid uptake induces metabolic and functional reprogramming of tumor-associated myeloid-derived suppressor cells. *Oncoimmunology.* 2017;6(10):e1344804.

64. Van den Bossche J, Baardman J, Otto NA, van der Velden S, Neele AE, van den Berg SM, et al. Mitochondrial Dysfunction Prevents Repolarization of Inflammatory Macrophages. *Cell Rep.* 2016;17(3):684-96.

65. Herber DL, Cao W, Nefedova Y, Novitskiy SV, Nagaraj S, Tyurin VA, et al. Lipid accumulation and dendritic cell dysfunction in cancer. *Nat Med.* 2010;16(8):880-6.

66. Shiraishi M, Shintani Y, Shintani Y, Ishida H, Saba R, Yamaguchi A, et al. Alternatively activated macrophages determine repair of the infarcted adult murine heart. *J Clin Invest.* 2016;126(6):2151-66.

67. Burzyn D, Kuswanto W, Kolodin D, Shadrach JL, Cerletti M, Jang Y, et al. A special population of regulatory T cells potentiates muscle repair. *Cell.* 2013;155(6):1282-95.

68. Arpaia N, Green JA, Moltedo B, Arvey A, Hemmers S, Yuan S, et al. A Distinct Function of Regulatory T Cells in Tissue Protection. *Cell.* 2015;162(5):1078-89.

69. Liu Q, Dwyer GK, Zhao Y, Li H, Mathews LR, Chakka AB, et al. IL-33-mediated IL-13 secretion by ST2+ Tregs controls inflammation after lung injury. *JCI Insight.* 2019;4(6).

70. Hancock WW, Thomson NM, and Atkins RC. Composition of interstitial cellular infiltrate identified by monoclonal antibodies in renal biopsies of rejecting human renal allografts. *Transplantation.* 1983;35(5):458-63.

71. Toki D, Zhang W, Hor KL, Liuwantara D, Alexander SI, Yi Z, et al. The role of macrophages in the development of human renal allograft fibrosis in the first year after transplantation. *Am J Transplant.* 2014;14(9):2126-36.

72. Zhao DX, Hu Y, Miller GG, Luster AD, Mitchell RN, and Libby P. Differential expression of the IFN-gamma-inducible CXCR3-binding chemokines, IFN-inducible protein 10, monokine induced by IFN, and IFN-inducible T cell alpha chemoattractant in human cardiac allografts: association with cardiac allograft vasculopathy and acute rejection. *J Immunol.* 2002;169(3):1556-60.

73. Salama M, Andrukhova O, Roedler S, Zuckermann A, Laufer G, and Aharinejad S. Association of CD14+ monocyte-derived progenitor cells with cardiac allograft vasculopathy. *J Thorac Cardiovasc Surg.* 2011;142(5):1246-53.

74. Oberbarnscheidt MH, Zeng Q, Li Q, Dai H, Williams AL, Shlomchik WD, et al. Non-self recognition by monocytes initiates allograft rejection. *J Clin Invest.* 2014;124(8):3579-89.

75. Eming SA, Wynn TA, and Martin P. Inflammation and metabolism in tissue repair and regeneration. *Science.* 2017;356(6342):1026-30.

76. Caputa G, Castoldi A, and Pearce EJ. Metabolic adaptations of tissue-resident immune cells. *Nat Immunol.* 2019;20(7):793-801.

77. Yellon DM, and Hausenloy DJ. Myocardial reperfusion injury. *N Engl J Med.* 2007;357(11):1121-35.

78. Frangogiannis NG. Inflammation in cardiac injury, repair and regeneration. *Curr Opin Cardiol.* 2015;30(3):240-5.

79. Dutta P, and Nahrendorf M. Monocytes in myocardial infarction. *Arterioscler Thromb Vasc Biol.* 2015;35(5):1066-70.

80. Wynn TA, and Vannella KM. Macrophages in Tissue Repair, Regeneration, and Fibrosis. *Immunity.* 2016;44(3):450-62.

81. Turnquist HR, Cardinal J, Macedo C, Rosborough BR, Sumpter TL, Geller DA, et al. mTOR and GSK-3 shape the CD4+ T-cell stimulatory and differentiation capacity of myeloid DCs after exposure to LPS. *Blood.* 2010;115(23):4758-69.

82. Miller AM, Asquith DL, Hueber AJ, Anderson LA, Holmes WM, McKenzie AN, et al. Interleukin-33 induces protective effects in adipose tissue inflammation during obesity in mice. *Circ Res.* 2010;107(5):650-8.

83. Molofsky AB, Nussbaum JC, Liang HE, Van Dyken SJ, Cheng LE, Mohapatra A, et al. Innate lymphoid type 2 cells sustain visceral adipose tissue eosinophils and alternatively activated macrophages. *J Exp Med.* 2013;210(3):535-49.

84. Jantsch J, Chakravortty D, Turza N, Prechtel AT, Buchholz B, Gerlach RG, et al. Hypoxia and hypoxia-inducible factor-1 alpha modulate lipopolysaccharide-induced dendritic cell activation and function. *J Immunol.* 2008;180(7):4697-705.

85. Bonilla WV, Frohlich A, Senn K, Kallert S, Fernandez M, Johnson S, et al. The alarmin interleukin-33 drives protective antiviral CD8(+) T cell responses. *Science.* 2012;335(6071):984-9.

86. Baumann C, Bonilla WV, Frohlich A, Helmstetter C, Peine M, Hegazy AN, et al. T-bet- and STAT4-dependent IL-33 receptor expression directly promotes antiviral Th1 cell responses. *Proc Natl Acad Sci U S A.* 2015;112(13):4056-61.

87. Rui T, and Tang Q. IL-33 attenuates anoxia/reoxygenation-induced cardiomyocyte apoptosis by inhibition of PKCbeta/JNK pathway. *PLoS One.* 2013;8(2):e56089.

88. Axtell AL, Fiedler AG, Chang DC, Yeh H, Lewis GD, Villavicencio MA, et al. The effect of donor age on posttransplant mortality in a cohort of adult cardiac transplant recipients aged 18-45. *Am J Transplant.* 2019;19(3):876-83.

89. Fan D, Takawale A, Lee J, and Kassiri Z. Cardiac fibroblasts, fibrosis and extracellular matrix remodeling in heart disease. *Fibrogenesis Tissue Repair.* 2012;5(1):15.

90. Hart A, Smith JM, Skeans MA, Gustafson SK, Stewart DE, Cherikh WS, et al. OPTN/SRTR 2015 Annual Data Report: Kidney. *Am J Transplant.* 2017;17 Suppl 1:21-116.

91. Duffy JP, Kao K, Ko CY, Farmer DG, McDiarmid SV, Hong JC, et al. Long-term patient outcome and quality of life after liver transplantation: analysis of 20-year survivors. *Ann Surg.* 2010;252(4):652-61.

92. Verleden SE, Ruttens D, Vandermeulen E, Bellon H, Van Raemdonck DE, Dupont LJ, et al. Restrictive chronic lung allograft dysfunction: Where are we now? *J Heart Lung Transplant.* 2015;34(5):625-30.

93. Krezdorn N, Lian CG, Wells M, Wo L, Tasigiorgos S, Xu S, et al. Chronic rejection of human face allografts. *Am J Transplant.* 2019;19(4):1168-77.

94. Mathews L, Lott J, Isse K, Lesniak A, Landsittel D, Demetris A, et al. Elevated ST2 distinguishes incidences of pediatric heart and small bowel transplant rejection. *American Journal of Transplantation.* 2016;16(3):938-50.

95. Townsend MJ, Fallon PG, Matthews DJ, Jolin HE, and McKenzie AN. T1/ST2-deficient mice demonstrate the importance of T1/ST2 in developing primary T helper cell type 2 responses. *J Exp Med.* 2000;191(6):1069-76.

96. Huleihel L, Hussey GS, Naranjo JD, Zhang L, Dziki JL, Turner NJ, et al. Matrix-bound nanovesicles within ECM bioscaffolds. *Sci Adv.* 2016;2(6):e1600502.

FIGURES:

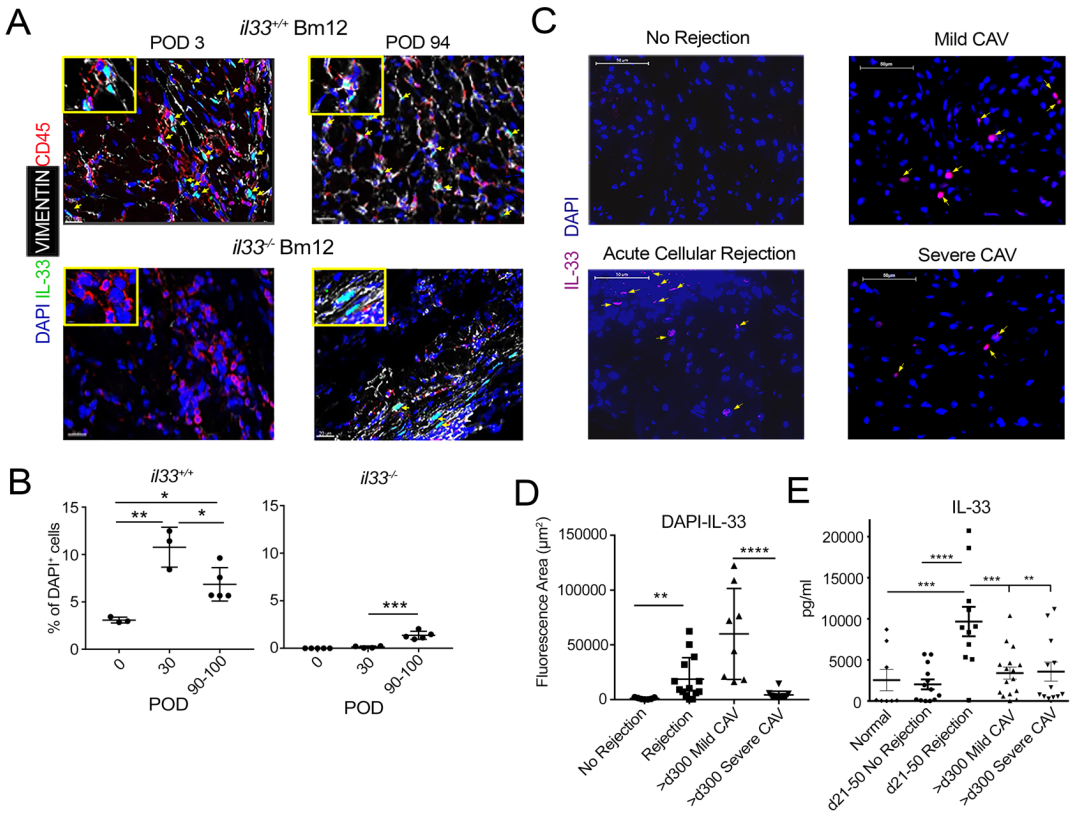

Figure 1: Augmented IL-33 is observed in allografts and the circulation during heart transplant rejection. (A-B) IL-33-expressing (*il33*$^{+/+}$) or IL-33-deficient Bm12 (*il33*$^{-/-}$) grafts were transplanted into wildtype (WT) C57BL/6 (B6) mice (n=3-5/group). **(A)** On post-operation day (POD) 3 or 90-100, grafts were evaluated by immunofluorescence staining for CD45 (red), Vimentin (white), IL-33 (green) and DAPI (blue). One representative image for each group is shown. Yellow arrows signify IL-33^{+} cells. Bar=20uM. **(B)** Quantitation of percentage IL-33^{+} cells in relation to the total number of DAPI^{+} cells. Graphs depict individual values and group mean±S.D. *P* values were generated using a one-way analysis of variance (ANOVA). **P*<0.05, ***P*<0.01, ****P*<0.005**. (C-D)** Increased graft IL-33 during acute clinical rejection and chronic rejection-associated coronary artery vasculopathy (CAV) was observed in analysis of endomyocardial biopsies (EMB) immunostained for IL-33 (magenta) and DAPI (blue). (**C**)

Representative image captures from EMB at time points diagnosed as rejection-free (Top Left Panel), suffering acute cellular rejection (ACR) (Bottom Left Panel), mild CAV (Top Right Panel), or severe CAV (Bottom Right Panel). Yellow arrows signify IL-33^{+} cells. Bar=50uM (**D**) Cohort mean for IL-33^{+}DAPI^{+} fluorescent area from EMB-samples at times of “No Rejection”; ACR or antibody-mediated “Rejection”, “Mild” or “Severe CAV” calculated for all readable EMB areas for each subject. ***P*<0.01 calculated via ANOVA. **(E)** Serum assessed for IL-33 by ELISA grouped by clinical status and time point of collection relative to transplantation. Graphs depict sample values and group means±S.E.M. P values by ANOVA. ***P*<0.01, ****P*<0.005C, *****P*<0.0001.

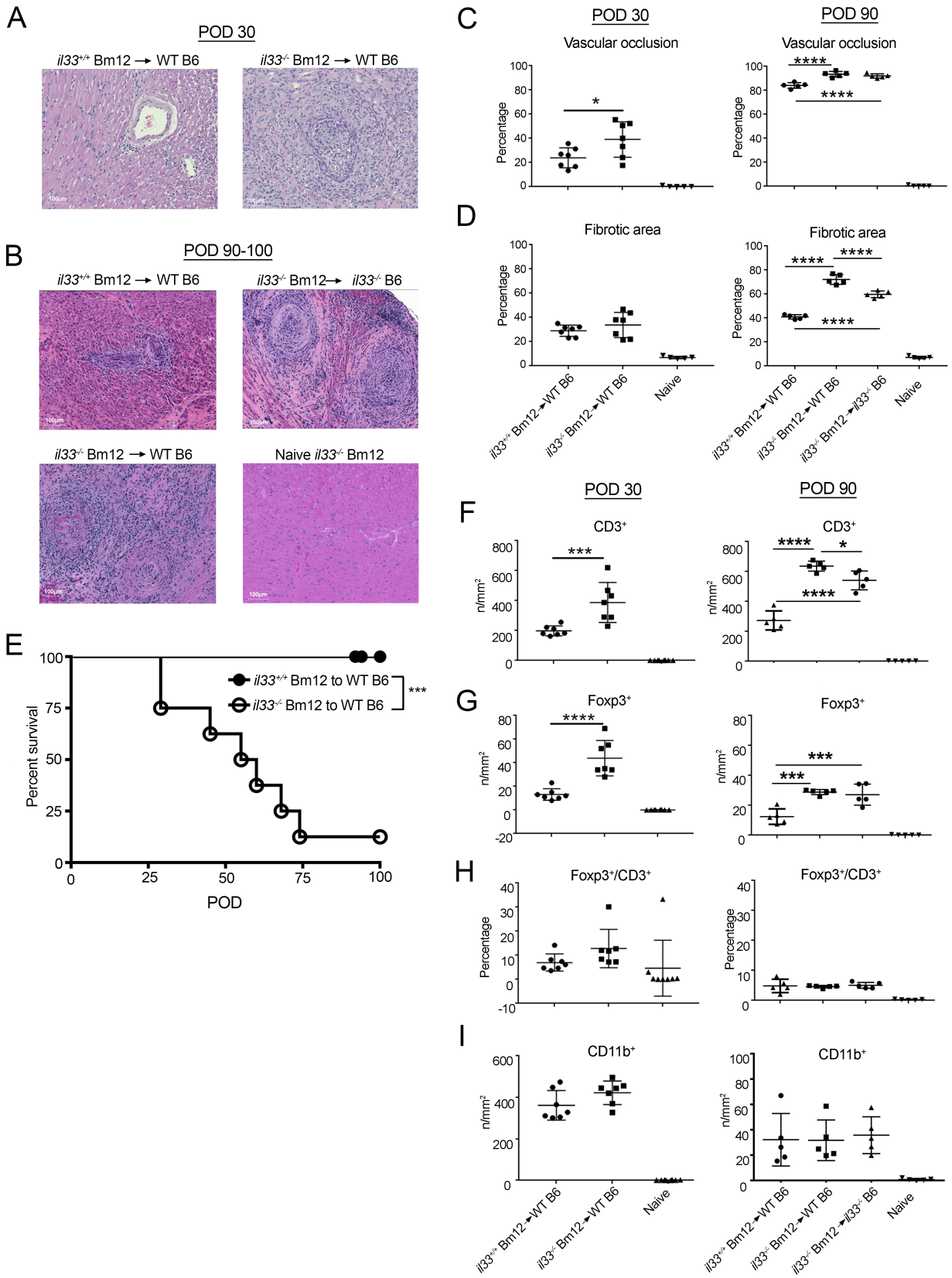
A
POD 30
il33+/+ Bm12 → WT B6
il33-/- Bm12 → WT B6
B
POD 90-100
il33+/+ Bm12 → WT B6
il33-/- Bm12→ il33-/- B6
il33-/- Bm12 → WT B6
Naive il33-/- Bm12
E
il33+/+ Bm12 to WT B6
il33-/- Bm12 to WT B6
***
Percent survival
POD
C
POD 30
POD 90
Vascular occlusion
Percentage
D
Fibrotic area
il33+/+ Bm12→WT B6
il33-/- Bm12→WT B6
Naive
il33-/- Bm12→il33-/- B6
F
CD3+
n/mm2
G
Foxp3+
H
Foxp3+/CD3+
I
CD11b+

Figure 2. The absence of graft IL-33 results in increased chronic rejection-associated vasculopathy, fibrosis, and T cell infiltration. IL-33-expressing (*il33*$^{+/+}$) or IL-33-deficient Bm12 (*il33*$^{-/-}$) grafts were transplanted into *il33*$^{+/+}$ or *il33*$^{-/-}$ B6 recipients (n=6-7/group). (**A-D**) Grafts harvested on POD30 and POD90-100 were evaluated after H&E staining for percentage vascular occlusion and fibrotic area quantified using NearCYTE. Graphs depict individual values and group mean±S.D. Naïve *il33*$^{-/-}$ Bm12 hearts were stained as controls. *P* values established by ANOVA. **P*<0.05, ***P*<0.01, ****P*<0.005, *****P*<0.0001**. (E)** Survival of *il33*$^{-/-}$ (n=10) versus *il33*$^{+/+}$ Bm12 grafts (n=7) in WT B6 recipients. *P* values by Kaplan-Meier analysis. ****P*<0.005. **(F-I)** Numbers of graft infiltrating CD3^{+}, Foxp3^{+} and CD11b^{+} cells identified using immunohistochemistry and quantified with NearCYTE. Graphs depict individual values and group means±S.D. *P* values calculated by ANOVA. **P*<0.05, ***P*<0.01, ****P*<0.005, *****P*<0.0001**.**

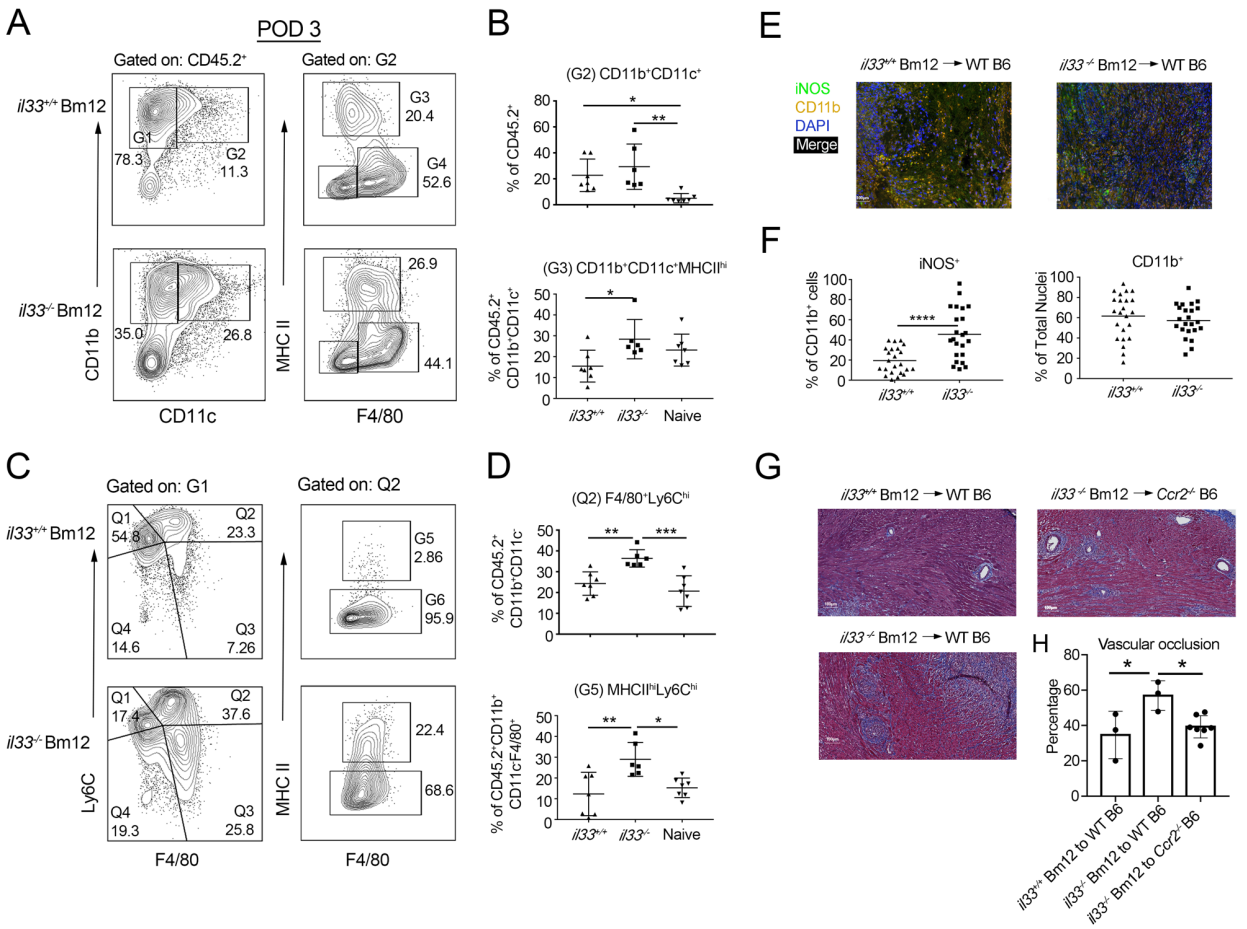

Figure 3. Increased iNOS^{+} inflammatory myeloid cells cause vasculopathy in IL-33-deficient heart transplants.

(**A-D**) Leukocytes infiltrating *il33*$^{+/+}$ or *il33*$^{-/-}$ Bm12 grafts transplanted into WT B6 recipients (n=6-7/group) were assessed by flow cytometric on POD3. Leukocytes from naïve Bm12 hearts were included as baseline controls (Naive; n=4). (**A**) Representative plots for monocyte-derived dendritic cell (monoDC) in the CD45.2^{+} gate. (**B**) Frequency of CD11b^{+}CD11c^{+} and CD11b^{+}CD11c^{+}MHCII^{hi} cells in the CD45.2^{+} gate. (**C**) Representative plots for macrophage subsets in the CD45.2^{+}CD11c^{-}CD11b^{+} gate. (**D**) Frequency of F4/80^{+}Ly6C^{hi}, F4/80^{+}Ly6C^{lo}, and F4/80^{+}Ly6C^{hi}MHCII^{hi} macrophages in CD45.2^{+}CD11c^{-}CD11b^{+} gate. *P* values calculated by ANOVA. **P*<0.05, ***P*<0.01, ****P*<0.005, *****P*<0.001. ***(E)*** Representative fluorescent immunolabeling for iNOS (Green) and CD11b (Orange) and DAPI (Blue) in *il33*$^{+/+}$ (left panel; n=5)

or *il33*$^{-/-}$ (right panel; n=6) Bm12 heart transplants into WT B6 recipients at POD30. Bar=100μM. *(F)* Quantification of %iNOS^{+}/CD11b^{+} and %CD11b^{+}/DAPI^{+} cells. Graphs depict 3-5 values for randomly selected regions from each transplant sample and group mean±S.D. *P* values were calculated with a two-tail *t*-test with Welch's correction. ****P<0.0001**. (G-H)** *il33*$^{+/+}$ or *il33*$^{-/-}$ Bm12 grafts were transplanted into B6 *WT* or *Ccr2*$^{-/-}$ recipients (n=3-7/group). Grafts harvested on POD30 were evaluated after Masson's Trichrome staining for (**G**) vasculopathy. (**H**) Percentage vascular occlusion was quantified, and graphs depict individual values and group mean±S.D. *P* values established using ANOVA. *P<0.05**.**

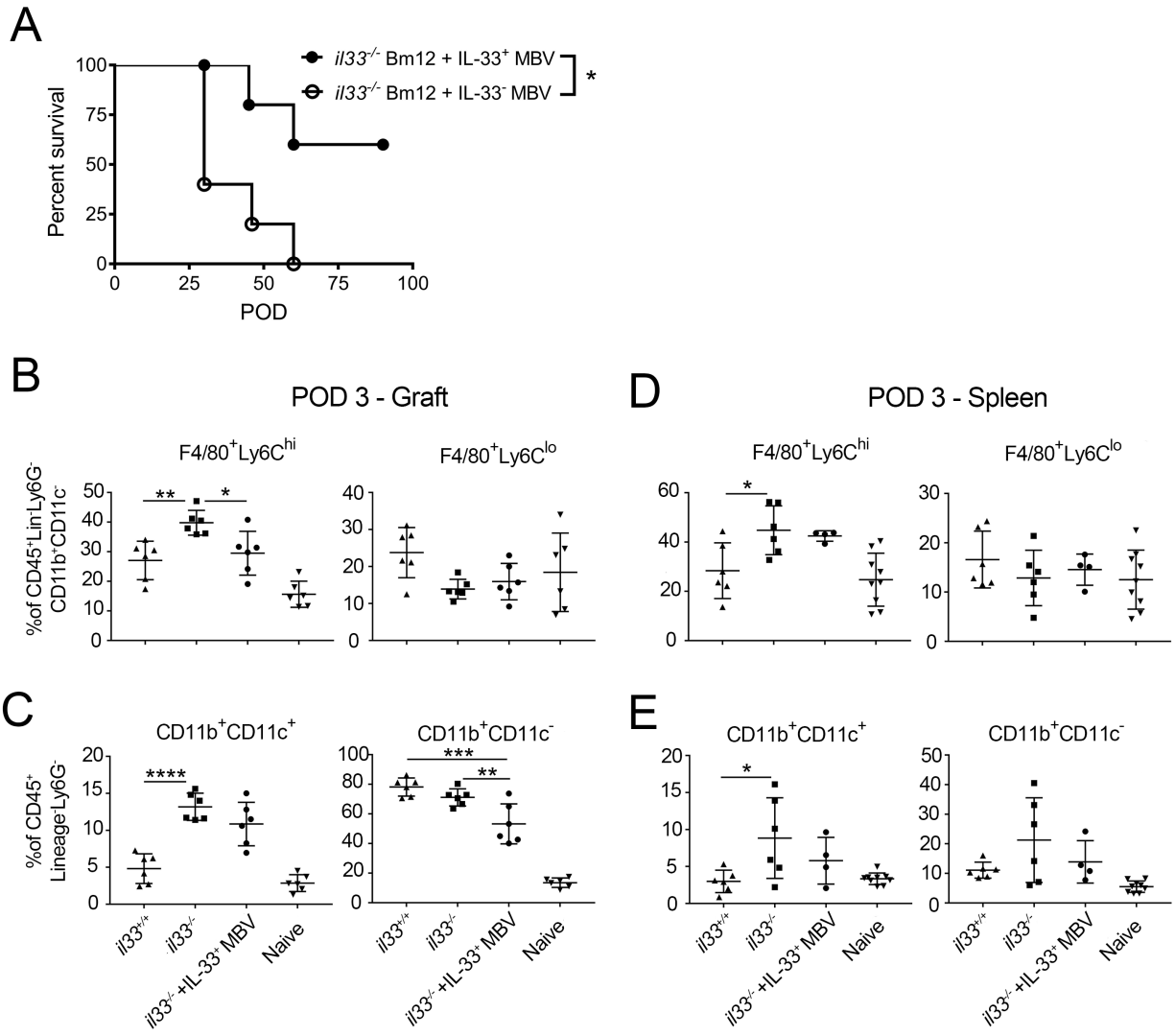

Figure 4. Restoring local IL-33 reduces inflammatory macrophages in the graft and limits chronic rejection of IL-33-deficient allografts.

Transplanted *il33*$^{-/-}$ Bm12 grafts were treated with matrix bound nanovesicles (MBV) generated from *il33*$^{-/-}$ (IL-33^{-} MBV) or *il33*$^{+/+}$ (IL-33^{+} MBV) B6 in hydrogel immediately after transplantation into *WT* B6 (n=6/group). (**A**) Survival of *il33*$^{-/-}$ Bm12 grafts treated IL-33^{+} MBV or IL-33^{-} MBV in WT B6 recipients. *P* values calculated by Kaplan-Meier analysis. *P<0.05. Graft infiltrating leukocytes (**B, C**) and splenocytes (**D, E**) at POD3 from additional groups of WT B6 recipients of *il33*$^{-/-}$ Bm12 grafts treated with IL-33^{+} MBV were compared using flow cytometry to those receiving

il33$^{+/+}$ Bm12 or *il33*$^{-/-}$ Bm12 grafts alone. Leukocytes from naïve Bm12 mice hearts and spleens were also included as controls (Naïve; n=6). Graphs depict individual values and group mean±S.D for F4/80^{+}Ly6C^{hi} and F4/80^{+}Ly6C^{lo} macrophages in the CD45.2^{+}CD3^{-}CD49b^{-}NK1.1^{-}CD90.2^{-}Ly6G^{-} CD11c^{-}CD11b^{+} population (**B, D**) and CD11b^{+}CD11c^{+} monoDC, and CD11b^{+}CD11c^{-} cells in the CD45.2^{+}CD3^{-}CD49b^{-}NK1.1^{-}CD90.2^{-}Ly6G^{-} population (**C, E**) in the graft and spleen, respectively. *P* values calculated using ANOVA. ****P<0.001, ***P<0.005, **P<0.01, *P<0.05.

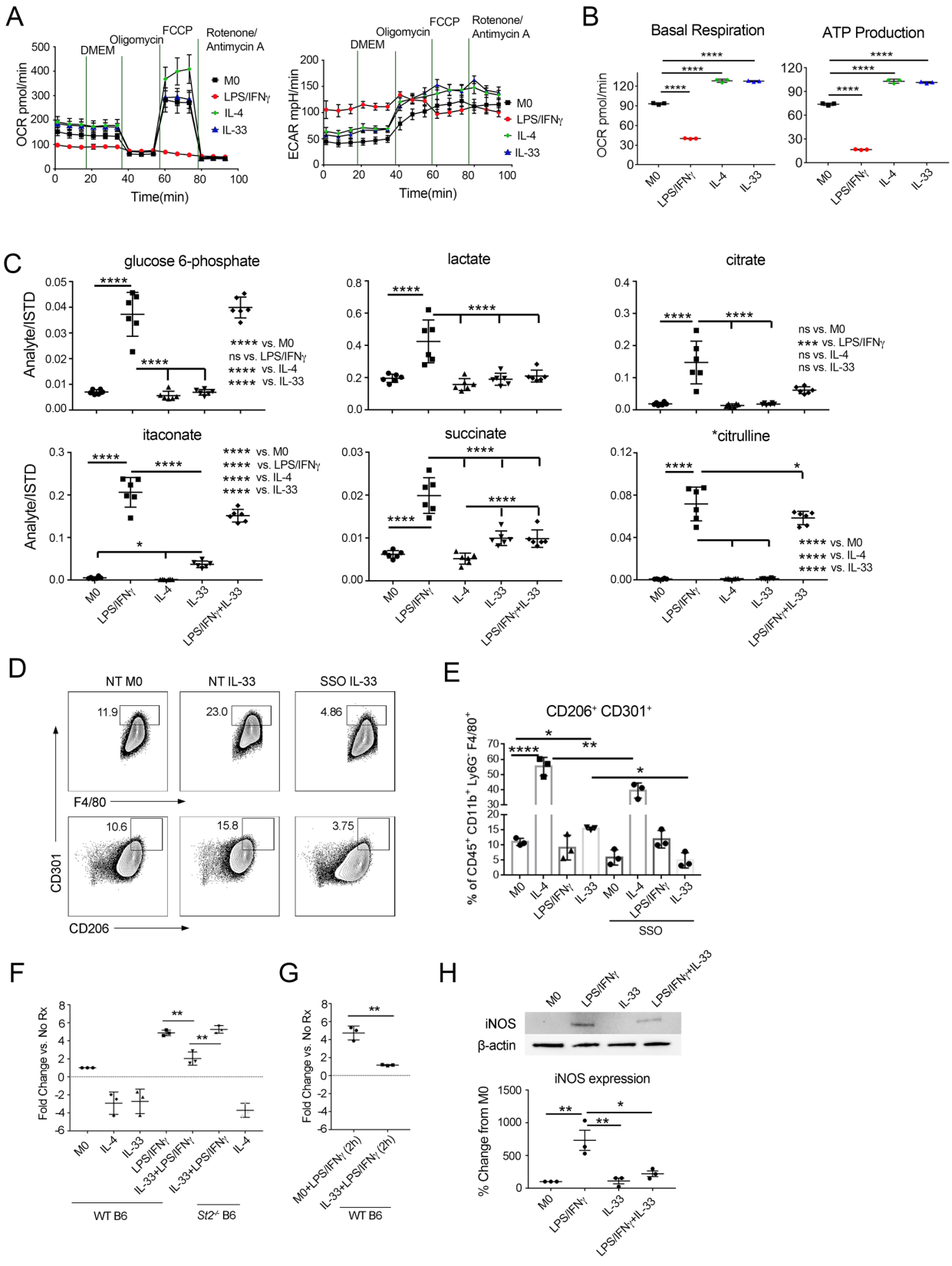
A
OCR pmol/min
DMEM
Oligomycin
FCCP
Rotenone/ Antimycin A
M0
LPS/IFNγ
IL-4
IL-33
Time(min)
ECAR mpH/min
B
Basal Respiration
ATP Production
C
glucose 6-phosphate
lactate
citrate
itaconate
succinate
*citrulline
Analyte/ISTD
**** vs. M0
ns vs. LPS/IFNγ
**** vs. IL-4
**** vs. IL-33
*** vs. LPS/IFNγ
ns vs. IL-4
ns vs. IL-33
LPS/IFNγ+IL-33
D
NT M0
NT IL-33
SSO IL-33
11.9
23.0
4.86
10.6
15.8
3.75
F4/80
CD301
CD206
E
CD206+ CD301+
% of CD45+ CD11b+ Ly6G- F4/80+
SSO
F
Fold Change vs. No Rx
M0
IL-4
IL-33
LPS/IFNγ
IL-33+LPS/IFNγ
IL-33+LPS/IFNγ
IL-4
WT B6
St2-/- B6
G
M0+LPS/IFNγ (2h)
IL-33+LPS/IFNγ (2h)
WT B6
H
iNOS
β-actin
iNOS expression
% Change from M0

Figure 5. IL-33 mediates a FA-dependent poising of macrophages for differentiation into a reparative and regulatory subset by promoting oxidative phosphorylation and negatively regulating iNOS expression.

(A) Oxygen consumption rate (OCR) and extracellular acidification rate (ECAR) were determined for B6 bone marrow-derived macrophages (BMDM) left untreated (M0) or stimulated with LPS+IFNγ, IL-4, or IL-33. One representative experiment of three independent experiments is shown. (**B**) Calculated mitochondrial basal respiration and ATP production for replicates from one experiment. ****P<0.0001, ***P<0.001. (**C**) Relative concentration (normalized to internal standard and cell number) of TCA metabolites or citrulline in lysates after overnight culture in media alone (M0) or media with LPS+IFNγ, IL-4, IL-33, or LPS+IFNγ+IL-33 determined using LC-HRMS. P values determined using ANOVA. *P<0.05, **P<0.01, ***P<0.005, ****P<0.001. n=6 samples/group. (**D-E**) Macrophages stimulated as above alone or with 200μM sulfosuccinimidyl oleate (SSO) for 24h were assessed for by flow cytometry. (**D**) Plots of $CD45^+CD11b^+Ly6G^-F4/80^+$ gated cells. (**E**) Frequency of $CD206^+CD301^+$ cells in the $CD45^+CD11b^+Ly6G^-F4/80^+$ gate. n=3 samples/group. P values calculated using ANOVA. *P<0.05, **P<0.01, ***P<0.005, ****P<0.001. (**F**) $F4/80^+$ macrophages from WT or $St2^{-/-}$ B6 mice were treated as in (G) before isolated RNA was assessed for *Nos2* by qRT-PCR. (**H**) WT B6 macrophages were first incubated with IL-33 overnight and then stimulated for 2 hours with LPS+IFNγ before RNA isolation and *Nos2* qRT-PCR. n=3 mice/group. Data are from one experiment and representative of two completed. *P* values calculated using ANOVA. **P<0.01. (**H**) Macrophages treated as in (C) were assessed by immunoblotting for iNOS. Quantification of immunoblotting mean pixel density was performed using ImageJ and loading was normalized to β-Actin (n=3). *P* values calculated by ANOVA. *P<0.05, **P<0.01.

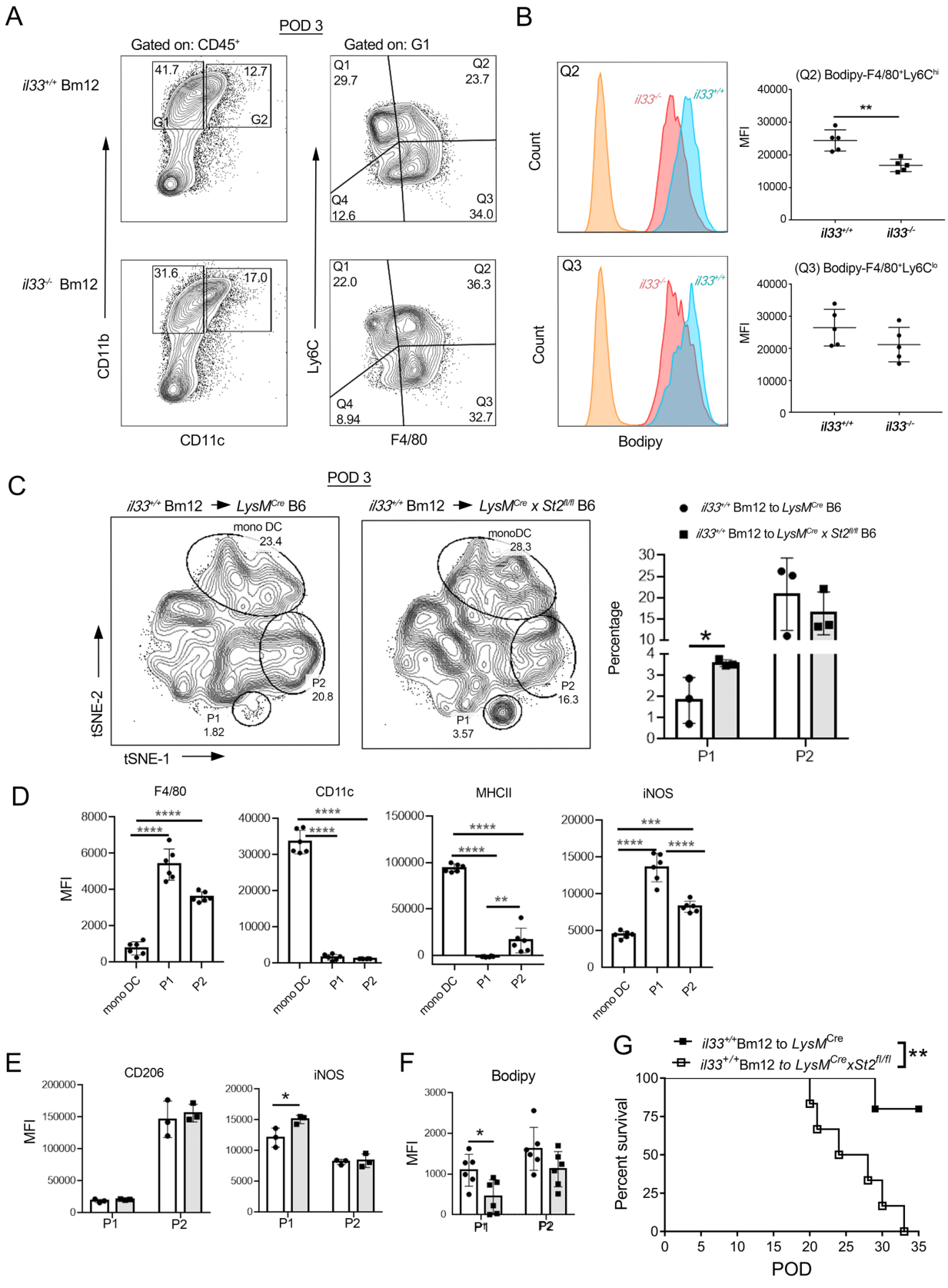
A
POD 3
Gated on: CD45+
Gated on: G1
il33+/+ Bm12
il33-/- Bm12
41.7
12.7
G1
G2
31.6
17.0
Q1 29.7
Q2 23.7
Q4 12.6
Q3 34.0
Q1 22.0
Q2 36.3
Q4 8.94
Q3 32.7
CD11b
CD11c
Ly6C
F4/80
B
Q2
Q3
Count
Bodipy
il33-/-
il33+/+
(Q2) Bodipy-F4/80+Ly6Chi
(Q3) Bodipy-F4/80+Ly6Clo
MFI
**
C
POD 3
il33+/+ Bm12 → LysMCre B6
il33+/+ Bm12 → LysMCre x St2fl/fl B6
mono DC 23.4
P2 20.8
P1 1.82
monoDC 28.3
P2 16.3
P1 3.57
tSNE-2
tSNE-1
il33+/+ Bm12 to LysMCre B6
il33+/+ Bm12 to LysMCre x St2fl/fl B6
Percentage
*
P1
P2
D
F4/80
CD11c
MHCII
iNOS
MFI
****
***
**
mono DC
P1
P2
E
CD206
iNOS
MFI
*
P1
P2
F
Bodipy
MFI
*
P1
P2
G
il33+/+Bm12 to LysMCre
il33+/+Bm12 to LysMCrexSt2fl/fl
**
Percent survival
POD

Figure 6. IL-33 targets intragraft myeloid cells to prevent rejection by upregulating their fatty acid uptake and limiting the generation of iNOS$^+$ pro-inflammatory macrophages.

(**A**) *il33*$^{+/+}$ or *il33*$^{-/-}$ Bm12 grafts were transplanted into WT B6 recipients (n=5/group). On POD3, flow cytometry of graft infiltrating leukocytes fatty acid uptake was assessed using Bodipy. (**B**) Bodipy uptake for Q2 (CD45$^+$CD11b$^+$CD11c$^-$F4/80$^+$Ly6C^{hi}) and Q3 (CD45$^+$CD11b$^+$CD11c$^-$ F4/80$^+$Ly6C^{lo}) populations. Graphs are individual values and group mean±S.D. *P* values were calculated using a two-tailed Student's t-test. **P*<0.05, ***P*<0.01, ****P*<0.005, *****P*<0.001. (**C-E**) *il33*$^{+/+}$ Bm12 grafts were transplanted into B6 *LysM*^{Cre} or *LysM*^{Cre}x*St2*$^{fl/fl}$ recipients. On POD3, graft infiltrating leukocytes were assessed by flow cytometry. (**C**) t-distributed stochastic neighbor embedding (t-SNE) contour plots generated from CD45$^+$CD3$^-$B220$^-$CD11b$^+$ gated cells (n=3 mice/plot). Population frequency (monoDC, P1, and P2) for each mouse from (C) in t-SNE plot. P values were calculated using a one-way ANOVA. **P*<0.05. (**D**) MFI for F4/80, CD11c, MHCII and iNOS for monoDC, pro-inflammatory (P1) and alternatively activated macrophages (P2) populations. (**E**) Comparison of MFI for CD206 and iNOS staining between P1 and P2 populations from *il33*$^{+/+}$ Bm12 grafts transplanted into B6 *LysM*^{Cre} (White) or LysM^{Cre}x*St2*$^{fl/fl}$ (Grey) recipients. Data are from one of two experiments completed. P values calculated using ANOVA. **P*<0.05, ***P*<0.01, ****P*<0.005, *****P*<0.001. **(F)** Bodipy uptake by indicated populations of graft infiltrating cells in B6 *LysM*^{Cre} (White) or LysM^{Cre}x*St2*$^{fl/fl}$ (Grey) recipients. Graphs depict individual values and group mean±S.D for CD45$^+$CD3$^-$B220$^-$CD11b$^+$ P1- and P2-gated cells (**G**) Survival of *il33*$^{+/+}$ Bm12 grafts transplanted into B6 *LysM*^{Cre} (White) or LysM^{Cre}x*St2*$^{fl/fl}$ recipients (n=5-6/group). *P* values calculated using Kaplan-Meier analysis. *P<0.05.